HHS Public Access

Author manuscript

Chemosphere. Author manuscript; available in PMC 2021 September 14.

Published in final edited form as:

Chemosphere. 2020 September ; 255: 126919. doi:10.1016/j.chemosphere.2020.126919.

Mitochondrial-related effects of pentabromophenol, tetrabromobisphenol A, and triphenyl phosphate on murine BV-2 microglia cells

Christine Bowen[1,*], **Gabrielle Childers**[1,*], **Caroline Perry**[1,*], **Negin Martin**[2], **Christopher A. McPherson**[1], **Tatlock Lauten**[1], **Janine Santos**[1], **G. Jean Harry**[1]

[1]National Toxicology Program Laboratory, National Institute of Environmental Health Sciences, Research Triangle Park, NC

[2]Neurobiology Laboratory, National Institute of Environmental Health Sciences, Research Triangle Park, NC

Abstract

The predominant reliance on bromated flame retardants (BFRs) is diminishing with expanded use of alternative organophosphate flame retardants. However, exposure related issues for susceptible populations, the developing, infirmed, or aged, remain given environmental persistence and home-environment detection. In this regard, reports of flame retardant (FR)-related effects on the innate immune system suggest process by which a spectrum of adverse health effects could manifest across the life-span. As representative of the nervous system innate immune system, the current study examined changes in microglia following exposure to representative FRs, pentabromophenol (PBP), tetrabromobisphenol A (2,2',6,6',-tetrabromo-4,4'-isopropylidine diphenol; TBBPA) and triphenyl phosphate (TPP). Following 18hr exposure of murine BV-2 cells, at dose levels resulting in ≥80% viability (10 and 40μM), limited alterations in pro-inflammatory responses were observed however, changes were observed in mitochondrial respiration. Basal respiration was altered by PBP; ATP-linked respiration by PBP and TBBPA, and maximum respiration by all three FRs. Basal glycolytic rate was altered by PBP and TBBPA and compensatory glycolysis by all three. Phagocytosis was decreased for PBP and TBBPA. NLRP3 inflammasome activation was assessed using BV-2-ASC (apoptosis-associated speck-like protein containing a CARD) reporter cells to

Correspondence: G. Jean Harry, NIEHS, P.O. Box 12233, MD E1-07, Research Triangle Park, NC 27709 USA.

*Current affiliation: CB: Emory University, Atlanta, GA; GC: University of Alabama, Birmingham, AL; CP: Perelman School of Medicine at the University of Pennsylvania, Philadelphia, PA, USA

Author contribution statement: Christine Bowen, Gabrielle Childers, and Caroline Perry conducted much of the experiments and were involved in the conceptualization of the study, Dr. Negin Martin designed and generated the BV2 ASC speck cells; Dr. Janine Santos established the cell-based assays for mitochondrial screening, Dr. G. Jean Harry contributed to the conceptualization and interpretation of the study and supervision of the experiments. Tatlock Lauten provided technical validation of the mRNA data and Dr. Christopher McPherson provided expertise for image analysis. All authors contributed to writing of the final manuscript. The authors wish to acknowledge the expert assistance of Dr. Guan Xie, Social & Scientific Systems, Durham, NC, for statistical analysis and Lois Wyrick for graphics. Drs. Will Gwinn and Kristen Ryan provided reviewer comments on the manuscript.

Declarations of interests: The authors declare that they have no known competing financial interests or personal relationships that could have appeared to influence the work reported in this paper.

visualize aggregate formation. PBP, showed a direct stimulation of aggregate formation and properties as a NLRP3 inflammasome secondary trigger. TBBPA showed indications of possible secondary triggering activity while no changes were seen with TPP. Thus, the data suggests an effect of all three FRs on mitochondria metabolism yet, different functional outcomes including, phagocytic capability and NLRP3 inflammasome activation.

Keywords

microglia; neuroinflammation; NLRP inflammasome; pro-inflammatory cytokines; lipopolysaccharide; flame retardants; neurotoxicity

1. Introduction

In general, flame retardants (FRs) represent four major categories based on their chemical composition: 1) inorganic, 2) nitrogen containing, 3) halogenated, and 4) organophosphate. For decades, halogenated FRs, including the brominated flame retardants (BFR), have been widely used in consumer products which has led to environmental contamination and human exposure (Birnbaum and Staskal, 2004). Use of specific classes of brominated FRs (BFRs) has been progressively phased-out or minimized worldwide; however, given their environmental persistence, concern remains for adverse human health effects (Stockholm Convention, 2017). Example BFRs include pentabromophenol (PBP) and the prevalent tetrabromobisphenol A (2,2’,6,6’,-tetrabromo-4,4’-isopropylidine diphenol; TBBPA). Recently, increased usage of alternative organophosphate flame retardants (OPFRs) such as, triphenyl phosphate (TPhP, also called TPP) has occurred (Abou-Donia et al., 2016; van der Veen and de Boer, 2012). As a general rule, human exposure to FRs is the result of exposure to components of commercial mixtures for example, Firemaster 550 (F550) is an additive FR formulation of brominated and aryl phosphate esters components used primarily in polyurethane foam. It was introduced as a major replacement product for the polybrominated diphenyl ether mixture, PentaBDE. Human exposure to FRs is thought to occur primarily by inhalation and ingestion (Mäkinen et al., 2009; Meeker et al., 2013) and PBP, TBBPA and TPP, or their metabolites, have been detected in human samples (Cariou et al., 2008; ECB, 2006; Shi et al., 2009; Sjödin et al., 2003; Smeds and Saukko, 2003; Thomsen et al., 2002) raising significant health issues given home environmental exposure (Castorina et al., 2017; Malliari and Kalantzi, 2017; Phillips et al., 2018; Stapleton et al., 2009) Currently, the majority of data available is for the BFR, TBBPA, and while there is limited data available for the alternative organophosphate flame retardants (OPFR) such as TPP, some similarities raise the possibility of subtle biological effects of exposure (Hendriks and Westerink, 2015; van der Veen and de Boer, 2012) that warrant further comparative examination. Despite TPP being a primary OPFR detected in house dust (Zheng et al., 2015; Stapleton et al. 2009), data on the potential for TPP to cause toxic effects in humans are limited and, in experimental animal models, toxicity has been reported with extremely high exposure (oral LD50: mouse - 1320 mg/kg; rat - 3800 mg/kg; Lewis, 2004). While environmental persistence of TPP is not as prevalent as for the BFRs, there is evidence of bioaccumulation in aquatic organisms. When zebrafish were examined for developmental toxicity, TPP and mono-substituted isopropylated triaryl phosphate induced

severe cardiac abnormalities (Du et al., 2015; McGee et al., 2013; Mitchell et al., 2018) Additional work in zebrafish showed altered ocular and neurodevelopment and muscular organization (Shi et al., 2018; 2019) that were independent of the aryl hydrocarbon receptor and a potential role of retinoic acid receptor was reported (Isales et al., 2015). Further work suggested metabolic disruptions in the zebrafish liver for TBBPA (De Wit et al., 2008) and TPP (Du et al., 2016). TPP has been reported to disrupt cellular energy metabolism and creatine synthesis in rats (Alam et al., 2012) and pyruvate metabolism and TCA cycle in mice (Wang et al., 2018) suggesting that such cellular effects were not species dependent.

Effects on the innate immune system have been reported following experimental exposure to BFRs. These effects manifest with the production of critical proteins or in cell functional dysregulation (Dietert, 2015; Takeshita et al, 2013). For example, successful pregnancy outcomes can be influenced by altered inflammatory regulation (Orsi and Tribe, 2008) and uterine immune activation has been reported following *in vivo* exposure of Wistar Han rats to TBBPA (250 mg/kg/day for 5 days; Hall et al., 2017). Additional evidence of an effect upon the uterus was provided in a 2-year carcinogenicity study where positive trends were observed in the incidences of uterine epithelial tumors (NTP, 2014). Based on evidence of TBBPA in human cord blood (Cariou et al., 2008), Arita et al. (2018) examined placenta explant cultures and reported elevated levels of the inflammatory cytokine, interleukin (IL)-6. Exposure also exacerbated the normal response to a bacterial challenge with elevated levels of IL-6 and tumor necrosis factor alpha (TNFα) and inhibition of heme-oxygenase 1 and IL-1β. Establishment of the placenta relies on proper regulation of inflammatory signaling in first-trimester trophoblasts and a dysregulation of IL-6, IL-8, and transforming growth factor beta has been reported in a human trophoblast cell line exposed to TBBPA (Park et al., 2014). A direct effect of TBBPA on immune cells has been observed with increased levels of TNFα and IL-1β in a rat pancreatic B cell line (Suh et al., 2017) and in murine macrophages (Han et al., 2009). In contrast, decreased levels of these cytokines were observed in peripheral blood mononuclear cells (Anisuzzaman and Whalen, 2016; Yasmin and Whalen, 2018) and natural killer cells (NK) (Anisuzzaman and Whalen, 2016) including a deficit in lytic function (Cato et al., 2014; Kibakaya et al., 2009). Overall, the pattern of response to TBBPA suggests alterations in the inflammatory response of various immune cells that could have significant health implications.

Recruitment of the innate immune system represents a coordinated cellular response to tissue damage in an effort to return the system to a homeostatic balance. The appropriate regulation of this process facilitates recovery while dysregulation can hinder this response and induce secondary injury. An adverse impact of TBBPA exposure on immune cell function has been demonstrated with the exacerbation of respiratory syncytial virus-induced pneumonia in perinatally-exposed mice (Takeshita et al., 2013; Watanabe et al., 2017). With inflammation, mitochondria play a multi-faceted role, including redox balance (Mills et al., 2017; Próchnicki and Latz, 2017). With TBBPA exposure, mitochondrial alterations and induction of redox pathways have been reported in immune cells (Park et al., 2019; Reistad et al., 2005; Suh et al., 2017) and disruptions in the tricarboxylic acid cycle and glycolysis in the medaka embryo (Ye et al., 2016). With TPP exposure, mitochondrial alterations have been reported in the liver (Chen et al., 2015) and in in zebrafish embryos (Lee et al., 2019). Overall, these findings suggest that TBBPA, and possibly TPP, can have effects on immune

cells that might be associated with altered mitochondrial function. If so, these effects may influence the ability of cells to respond to an immunological or physical insult (Wantanabe et al., 2017) and represent a compromised system.

Alteration in immune cells may represent a basis for developmental neurotoxicity. In the nervous system, microglia serve as the resident mononuclear phagocytes that respond to intrinsic and extrinsic factors, leading to changes in cell function and responsiveness (for review, Sominsky et al., 2018). In this function microglia play a critical role in multiple processes (Harry and Kraft, 2012; Thion and Garel, 2017) not only with injury but also during CNS development including, neurovascularation (Harry and Pont-Lezica, 2014), neural cell differentiation (Erblich et al., 2011), neural migration (Aarum et al., 2004), and synaptic pruning and sculpting (Schafer et al., 2012). Thus, alterations in the function of these cells can significantly contribute to neurotoxicity during development and across the life-span. The largest body of data on neurotoxicity for FR is for TBBPA. Examination of an acute exposure in mice at 3 hr, the time of peak levels of TBBPA in the plasma (Schauer et al., 2006), reported conflicting effects on behavior between 0.1 and 5 mg/kg body weight with no effects observed at 250 mg/kg (Nakajima et al., 2009). The vulnerability of the developing nervous system has been implicated as a primary issue for BFR exposure (Dingemans et al., 2011). Assessment of neuropathology and neurobehavior in a standard two-generational study showed no overt evidence of neurotoxicity up to 1000 ppm (Cope et al., 2015). Developmental exposure to TBBPA administered during critical windows of postnatal brain development showed no overt behavioral effects in the adult mouse (Eriksson et al., 2011) yet a minor effect on synaptic activity (Hendriks et al., 2015). With the inclusion of gestational exposure, subtle effects of TBBPA have been reported. In weanling mice exposed to TBBPA (1000 or 10,000 ppm) from gestational day 10 through postnatal day 20, an elevation in the number of NeuN+ neurons in the hilus of the hippocampus and an increase in apoptotic bodies in the neurogenic sub-granular zone were reported, suggestive of a disruption in neurogenesis (Saegusa et al., 2012). In agreement with this was the deficit observed in the successful maturation of newly generated hippocampal neurons (Kim et al., 2017). This deficit was accompanied by changes in a hippocampal dependent memory task, decreased brain derived neurotrophic factor levels, and increased immunostaining for astrocytes and microglia (Kim et al., 2017). Given that microglia regulate the generation and survival of healthy new neurons in the hippocampus through phagocytosis of apoptotic neuroprogenitor cells (Sierra et al., 2010), changes in the function of these cells may have contributed, not only to the increase in developing neurons (Saegusa et al., 2012), but also the increased presence of apoptotic bodies in the SGZ due to lack of phagocytic clearance. The overall effect could contribute to the decrease in successful maturation and integration of these neurons into the hippocampus (Kim et al., 2017).

In vitro screening of TBBPA across a number of proposed neurotoxicity models showed a decrease in cell viability and differentiation in a mouse stem cell differentiation assay at 50 μM for 4 days with no effects observed at dose levels ≤25 μM. Human neuroprogenitor cell proliferation and primary rat neurite outgrowth were not affected and human-derived neurite outgrowth was altered at dose levels that decreased cell viability [10 – 30 μM] (Behl et al., 2015). In human iPSC-derived neural 3D cultures comprised of neurons and astrocytes, cytotoxicity was not observed until dose levels >50 μM for 6 days or >100 μM for ≤2

days (Liang et al., 2019). Cell functional alterations were observed for TBBPA and TPP at >30 μM with a decrease in peak intracellular $Ca2^{+}$ oscillations. In comparison, mouse cortical and hippocampal primary neurons showed apoptotic changes at levels as low as 10 μM within 6–24 hr (Szychowski and Wójtowicz, 2016; Wójtowicz et al., 2014) as did cerebellar primary cells (Lenart et al., 2017). The *in vitro* models previously used to assess neurotoxicity of FRs have been devoid of microglia and thus, innate immune influences. Based on findings from neuronal or neuronal/astrocyte cultures, the primary modes of action identified include calcium homeostasis, thyroid hormone receptor activation, NOTCH signaling, and possibly, an oxidative stress response (Al-Mousa and Michelangeli, 2012; Diamandakie et al., 2019; Hendriks et al., 2012, 2015; Reistad et al., 2007; Zieminska et al., 2015, 2017). While the focus is often on neurons, these processes are also critical in the maturation, activation, and regulation of microglia (Brawek et al., 2017; Lima et al., 2001; Noda, 2015). Thus, to determine if FRs (PBP, TBBPA, and TPP) can manifest a direct action on brain immune cells, we examined responses in a murine microglia cell line. We examined the stimulation of a pro-inflammatory response, altered response to inflammatory stimuli and, changes in mitochondrial bioenergetics and report findings to suggest that FR exposure can modify brain immune cells.

2. Materials and Methods

2.1 Dosing Solutions

Stocks (100 mM) of triphenyl phosphate (TPP 115–86-6; 241288), 3, 3’, 5, 5’ tetrabromobisphenol A (TBBPA 79–94-7; 330396), pentabromophenol (PBP 608–71-9; P1608) (Sigma-Aldridge, St. Louis, MO) were prepared in 100% DMSO and stored at 4°C. All dosing solutions were prepared in DMEM from stocks immediately prior to dosing for final dosing concentration of 40 μM or 10 μM and 0.0004% DMSO. Stocks were prepared of ultrapure lipopolysaccharide (LPS; 1 endotoxin unit (EU)/ng, E. coli 055:B5 Lot#4231A1 List Biological Laboratories, Campbell, CA) with sonication in nuclease free sterile water. Stocks of adenosine 5’-triphosphate disodium salt hydrate were prepared in sterile dH_2O (ATP; 100 mM; Sigma Life Science; St. Louis, MO). Stocks were stored at −20°C.

2.2 Cell Culture

BV-2 cells were maintained in DMEM (#11995–065 Gibco, 94.5 g/L glucose, 2 mM L-glutamine ThermoFisher, Waltham, MA) supplemented with 10% Fetal Bovine Serum (FBS; #100–106 0.25 endotoxin units (EU)/mL; Gemini Bio-Products, Sacramento, CA), 100 U/mL penicillin and streptomycin (#P0781 Sigma-Aldrich, Burlington, MA). Unless otherwise stated, cells were plated in tissue culture plates (Corning, Corning, NY) at the following densities: 96-well (32,500 cells/cm^2), 24-well (150,000 cells/cm^2), 6 or 12-well (105,000 cells/cm^2) and allowed to adhere for 24 hr prior to exposure. Thermo-Fisher black-walled optical plates were used for experiments requiring imaging or densitometry. Cells were maintained at 37°C, 5% CO_2/5% O_2, 90% humidity (Nu-5831 tri-gas incubator, Nuaire, Plymouth, MN).

2.3 Cell Viability

To ensure that the responses observed would not be directly related to cell death, cell viability was initially assessed at multiple dose level and times to select experimental conditions. To allow time for changes in metabolism, mRNA response, and protein production an exposure time of 18h hr was selected Cell viability was determined using CyQuant Direct Cell Proliferation Assay (Molecular Probes, Eugene, OR) following manufacturer's instructions. Cells (24-well plate) were exposed to PBP, TBBPA, or TPP (5, 10, 20, 40 μm) for 18 hr, then incubated for 1 hr with 10 μL of 10x dye (100 μL DMEM, 50 μL nucleic acid stain, 250 μL background suppressor I). Fluorescence measurements were taken at 480 nm excitation and 535nm emission using a Tecan infinite M200PRO plate reader (Tecan, Mannedorf, Switzerland). Live cell number was estimated based upon standard curve and calculated as percentage of control.

2.4 Nitrite Production

Nitrite accumulation in culture medium was measured as an indirect indicator of nitric oxide synthesis using a GREISS Reagent kit (Promega, Madison, WI) following manufacturer's instructions. BV-2 cells (12-well plate) were exposed to PBP, TBBPA, or TPP (10 or 40 μM) for 18 hr. A 50 μL aliquot of a total 100 μL cell media was placed in a clear 96-well enzymatic assay plate (Costar, Washington, D.C.), 50 μL of sulfanilamide solution added, and held at room temperature (RT) in the dark for 10 min. *N*-1-napthylethylenediamine (50 μL) was added (RT; dark; 10 min). Absorbance at 548 nm was recorded in a BioTek Synergy 4 plate reader using GenBio software. Background (ultra-pure deionized water and complete DMEM media) corrected data was plotted relative to nitrite standard curve.

2.5 Mitochondrial Assessments

BV-2 cells were plated in a Seahorse XFe96 microplate (Agilent Technologies, Santa Clara, CA) at 5,000–7,000 cells/well in 80 μL of DMEM (4.5g/ D-glucose, 2.5 mM L-glutamine without antibiotics, supplemented with 10% FBS) and allowed to adhere for 1 hr followed by the addition of 120 μL of DMEM (without FBS) and incubation for 24 hr. Cells were then exposed to vehicle, PBP, TBBPA, or TPP (10 μL or 40 μL) for 18 hr. Cells were gently washed with 180 μL phenol free buffered (5mM HEPES) Seahorse XF media supplemented with 4.5 g/L glucose, 2 mM L-glutamine, and 1 mM sodium pyruvate, pH of 7.4. Cells were maintained under ambient air conditions for 1 hr at 37°C. Seahorse sensor cartridges were hydrated and loaded to deliver a final concentration of 50mM 2-deoxyglucose and 0.5μM rotenone for the glycolytic rate assay or 0.9μM oligomycin, 0.75 μM carbonyl cyanide-4-(trifluoromethoxy)phenylhydrazone (FCCP), and 1 μM rotenone for the mitochondrial stress test. Oxygen consumption rate (OCR) and extracellular acidification rate (ECAR) were measured using the XFe96 Seahorse Bioanalyzer (Agilent Technologies). Proton efflux rate (PER) for glycolytic rate was calculated using Wave Software (Agilent Technologies). Cells were stained with 20 μL (200μg/mL) Hoechst 33342 dye post-run for 5 min, imaged (ImageXpressTM Micro Confocal; Molecular Devices, San Jose,CA) and cell counts determined using the Find Blobs feature of MetaExpress Software's Count Nuclei Application. Data was normalized to cell number.

As a supporting confirmation of the effects observed in the seahorse bioanalyzer experiments, a specific cell line, the isogenic osteosarcoma cell line 143B (gift from Eric Schon, Columbia University, NY), was used as an experimental tool. This cell line carries the full complement of mitochondrial DNA (mtDNA; rho+) and can generate ATP through mitochondrial oxidative phosphorylation (OXPHOS) or glycolysis and the mtDNA-depleted counterpart (rho0) can only grow through glycolysis. Cells were maintained in DMEM (Gibco #11965–092; 4.5 g/L glucose) supplemented with 10 mM pyruvate (Sigma #S8636), 50μg/ml uridine (Sigma, #U3003), 10% FBS (Hyclone #SH30070.03), 1% penicillin/streptomycin (Gibco) under incubated conditions (37°C; 5% CO_2/5% O_2, 90% humidity). Cells were trypsinized (0.25%) and seeded at 6,000 cells/well in an opaque-walled 384-well tissue culture plate (Corning) and allowed to adhere for 24hr. Cells were exposed to vehicle and multiple concentrations of test compounds (PBP, TBBPA, and TPP) for 24 hr. Prior to and immediately following exposure, cell density in individual wells was confirmed by an IncuCyte S3 live-cell analysis system (Essen BioScience Inc., Ann Arbor, MI). Total cellular ATP levels was determined by CellTiter-Glo^R (Promega) following manufacturer's instructions. Luminescence was detected using a Clariostar plate reader (BMG Labtech). Data were expressed as fold-change relative to vehicle-treated controls. Rotenone, a known mitochondrial complex I inhibitor, was used as an assay positive control.

2.6 qRT-PCR

Total RNA from BV-2 cells exposed to FRs for 18 hr was isolated using TRIzol® Reagent (Invitrogen, Carlsbad, CA), quality assessed by NanoDrop (Thermos Scientific, Wilmington, DE), and complementary deoxyribonucleic acid (cDNA) synthesized from 2.5 μg total RNA using SuperScript™ II reverse transcriptase with random hexamers (Invitrogen). qPCR was performed in duplicate using a QuantStudio 7 Flex Real-Time PCR System (Applied Biosystems; Foster City, CA) with TaqMan® detection of reaction products. A 2.5 μL cDNA template was added with 1X Power TaqMan® Universal PCR Master Mix (ThermoFisher Waltham, MA). The 20 μL PCR reaction mixtures were held at 50°C for 2 min, 95°C for 10 min, followed by 40 cycles at 95°C for 15 s and 1 min at 60°C. Amplification curves were generated with QuantStudio™ 6 and 7 Flex Real-Time PCR System Software v1.0 (Applied Biosystems). Data was obtained from samples that met inclusion criteria of transcript detection at <32 cycles. mRNA levels were calculated relative to *Gapdh.* and compared to vehicle control using the $2^{-\Delta\Delta CT}$ method.

2.7 TNFα ELISA

Mouse TNFα ELISA MAX kit (BioLegend, San Diego, CA) with BD OptEIA Reagent Set B was used for analysis of protein released into 1 mL total medium from BV-2 cells (4×10^5 cells; 6 well plate) following FR exposure (10 μM or 40 μM) for 18 hr following manufacturer's instructions. Briefly, a capture antibody (100μL; 1:250 in coating buffer) was added to a 96-well flat bottom plate (Thermo Fisher Scientific, Rochester, NY) and held overnight at 4°C, then washed with buffer and held at RT for 1 hr. A 100μL aliquot of 40x diluted sample was added and incubated at RT for 2 hr. Wells were washed and 100 μL detection antibody (1:500) added for incubation (RT; 1 hr). Following a sequence of washes, wells were incubated by a sequence of 100μL streptavidin-HRP antibody (1:250; RT; 30 min), 100 mL substrate solution (RT; dark; 30 min) then 50 μL stop solution.

Optical density values were determined at 450nm with a 570nm background subtraction in a BioTek Synergy 4 plate reader. Protein levels were determined based on a recombinant protein standard curve and the total amount of protein from each well was calculated to total medium volume and cell counts.

2.8 IL-1 Production

To determine if exposure to the FR could directly stimulate a proinflammatory cytokine response HEK Blue™ IL-1R cells (InvivoGen, San Diego, CA) were used to determine the release of bioactive IL-1 (α and β) by the activation of the IL-1 receptor. Binding of the IL-1R triggers a signaling cascade leading to NF-κB activation and production of a secreted alkaline phosphatase (SEAP) reporter gene under the control of an IFN-γ promoter fused to NF-κB and AP-1 binding sites. SEAP is then assessed using QUANTI-Blue™ with a detection range of 1pg/mL-100 ng/mL. The release of IL-1 by BV-2 cells following exposure was assessed following manufacturer's instructions. Briefly, HEK Blue™ cells were maintained in growth medium containing DMEM phenol-free media (4.5 g/L glucose, 2 mM L-glutamine; 11965–092 Gibco, Gaithersburg, MD) supplemented with 10% FBS and the addition of 50 U/mL penicillin, 50μg/mL streptomycin, 100μg/mL Normocin, 200 μg/mL hygromycin B Gold, 1 μg/mL puromycin, and 100 μg/mL Zeocin (Invivogen). HEK Blue™ cells were resuspended in test medium (growth medium in the absence of hygromycin, puromycin, and zeocin) and a 180 μL aliquot (50,000 per well/96 well plate) was incubated overnight at 37°C in 5% CO_2.with a 20 μl aliquot of BV-2 cell conditioned medium (collected from a total volume of 1 mL from a 6-well plate) following FR exposure for 18 hr. A 20 μL aliquot of medium from each well was added, in duplicate, to a 96-well enzymatic plate, 180 μL Quanti-Blue reagent (InvivoGen) added, and incubated (37°C; 1 hr). Assay controls included recombinant IL-1 and TNF-α protein. Absorbance measurements at 630nm were recorded using a Clariostar plate reader (BMG Labtech, Ortenburg, Germany). Data was calculated relative to vehicle control.

2.9 Response to LPS Challenge

To determine if exposure to each of the FRs would alter the response of microglia to a pro-inflammatory stimulus, the response following LPS was examined. BV-2 cells were exposed to each FR at the lower dose level 10 μM for 15 hr then challenged with the addition of LPS (100 EU/mL) for 3 hr. Samples were examined for elevations in mRNA levels for *Tnfa, Il1a,* and *Il1b*.

2.10 Phagocytosis of Bioparticles

Phagocytic capability was measured by dosing with PHrodo Red E. Coli Bioparticles conjugate for phagocytosis (Life Technologies, Eugene, Oregon, #P35361, LOT#2024790). BV2 cells were plated in an Optical 96 well plate in phenol-free supplemented DMEM and allowed to adhere for 24 hr. Following a 50% media change to non-supplemented DMEM, cells were exposed to 10μM PBP, TBBPA, or TPP for 18 hr. As an assay control, cells were incubated for 30 min with the phagocytosis inhibitor, cytochalasin D (10 μM; Life Technologies, PHZ 1063, LOT#5675843A). Cells were then exposed to various final concentration of bioparticles (0, 10, 25, or 50 μg/mL) for 1.5 hr. Cells were washed with PBS then fixed in 4% paraformaldehyde/0.1M phosphate buffer (PB)

for 30 min followed by 2x PBS washes. Microglia were visualized by immunostaining with rabbit poly-clonal anti-Iba-1 (1:800, 24 hr, 4°C, Wako Biolaboratories, 019–19741) followed by Alexa-488-conjugated goat anti-rabbit antibody (1:5000, 1 hr, RT; Jackson ImmunoResearch, Jacksonville, PA, USA), rinsed with PBS, then incubated with DAPI (1:50000, 5 min, RT; Invitrogen, Carlsbad, CA, #D3571). Following PBS rinse, cells were visualized (ImageXpress™ Micro Confocal; Molecular Devices, San Jose, CA). Four defined regions of interest within each well (equal size and well-location) were used for imaging of phagocytic particles co-localized within Iba-1+ cells. Within the MetaXpress software, a custom module was designed to identify particles inside cells and number of microglia within each region. The fluorescent intensity of particles phagocytized by BV2 was determined.

2.11 NLRP3 Inflammasome Activation

The nucleotide-binding oligomerization domain–(NOD-) like receptor 3 (NLRP3) activation is induced by a variety of endogenous triggers (Hughes and O'Neill, 2018; Strowig et al, 2012). The sensor molecule of NLRP recruits the adaptor protein, apoptosis-associated speck-like protein containing a CARD (ASC) and the cysteine protease caspase-1. The resulting protein aggregate, termed "ASC speck", promotes the activation of caspase-1 and initiates cleavage of inactive precursor molecules of the IL-1β cytokine family to mature proteins that are involved in a series of immune and inflammatory processes. For real-time imaging of NLRP3 inflammasome activation, a reporter BV-2 ASC cell line was generated. HEK293T/17 cells (ATCC # CRL-11268) were transiently transfected with pMD2G (#12259, Addgene, Cambridge, MA), pUMVC (#8449; Addgene) and retroviral transfer vector pRP-ASC-ESCBLerulean (Addgene #41840) using Lipofectamine 2000 (ThermoFisher Scientific) adapting the method of Salmon and Trono (2006). Forty-eight hr post-transfection, supernatant was used for transduction of BV-2 cells following the method of Stutz et al. (2013) to create an ASC reporter cell line. Titers were determined by qPCR for integration of retroviral particles into host genome, titration of virus co-expressing fluorescent moieties was conducted via flow cytometry, and clonal cell lines were derived from infected polyclonal BV-2 cells. Cell culture conditions were identical to normal BV-2 cells. BV-2-ASC cells were exposed to PBS or LPS (33 ng/mL) for 3hr followed by a ¾ media change prior to the addition of vehicle or compound (10 μM TBBPA, PBP, or TPP). As an assay positive control, LPS-primed cells were exposed to ATP (5 mM: 30 min). Cells were immediately placed in an IncuCyte S3 live-cell analysis system under normal incubator conditions. Images were captured using IncuCyte ZOOM 2015A software (5-min intervals for 40 min; 1-hr intervals for 24 hr) and formation of ASC aggregates was determined based upon methods of Stutz et al. (2013) distinguishing between diffuse fluorescent cytoplasmic signals and distinct aggregations. Using Fiji ImageJ software (Schindelin et al. 2012), regions of interest (ROI) were identified within each well, standardized by total number of cells, threshold set for Speck size and intensity, and the number of SPECKS within each determined.

2.12 Statistical Analysis

Statistical analyses were performed using GraphPad Prism software (GraphPad Software, Inc., San Diego, CA). Bartlett's test was used to test for homogeneity of variance.

In experiments where LPS/ATP was used as assay positive control to confirm assay performance, the data was not included in the analysis. Results are expressed as standard error of mean or 95% confidence intervals as indicated. Experimental n size is stated in figure legends and all experiments were replicated. Data from experiments comparing across dose levels for each FR in non-LPS primed BV-2 and in rho+ and rho0 cells were evaluated using a one-way ANOVA. Data from experiments examining the response of cells to LPS following FR exposure or in assessing the inflammasome response to compounds in cells primed with LPS were analyzed by a two-way ANOVA with dose and LPS as factors. Independent group mean comparisons were conducted with Tukey's or Dunnett's multiple comparisons tests. Data that did not meet homogeneity of variance criteria was analyzed by a Kruskal-Wallis test followed by a Dunn's multiple comparisons test. For Normalized Basal Respiration, ATP linked Respiration, Maximum Respiration and Mean Basal Glycolytic Rate, data was analyzed by a two-way ANOVA with dose and chemical as factors. Post hoc comparisons were conducted for each chemical on each dose group (10uM and 40uM) as compared to control. p values were adjusted using Hommel's method for multiple comparisons (Hommel, 1988). For Compensatory Glycolysis, dose effects were assessed using the Kruskal-Wallis rank sum test on individual chemicals followed by a Wilcoxon Rank sum test for pairwise comparisons to the control, adjusted using Hommel's method. Sample n sizes are provided in figure legends and all experiments were replicated.

3. RESULTS

3.1 Cell viability

At 18 hr of exposure, cell viability remained within the range of controls for PBP and TBBPA at doses up to 40 μM (Fig. 1A). For TPP, viability was not altered at the 10 μM dose level but was slightly lower (approximately 18%) at 40 μM, as compared to controls ($p<0.001$; Fig. 1A).

3.2 Nitrite Production

BV-2 cells can be induced by the pro-inflammatory stimulus, LPS, to produce nitrite. With exposure to PBP, TBBPA, or TPP, nitrite accumulation in culture medium was not significantly altered suggesting limited activation of oxygen radicals in the oxidization of nitric oxide (Fig. 1B).

3.3 Mitochondrial Bioenergetics

To determine if exposure to the test compounds would alter mitochondrial bioenergetics, mitochondrial function was monitored real-time in cells exposed to PBP, TBBPA, or TPP using the Seahorse Bioanalyzer. Oxygen consumption rate (OCR) and extracellular acidification rate (ECAR) were monitored over the course of sequential additions of mitochondrial stressors, i.e., oligomycin, FCCP, and rotenone (Fig. 2A). Addition of oligomycin, an inhibitor of mitochondrial ATP synthase, reports the fraction of ATP production that is linked to respiration thus informing on the level of proton leak or coupling of the respiratory chain. FCCP is an ionophore that dissipates the mitochondrial membrane potential. Changes in oxygen consumption after FCCP addition reflect the cell's maximal respiratory capacity. Rotenone and antimycin inhibit complex I and III, respectively, shutting

down electron flow and thus, respiration. Basal respiration, ATP-linked respiration, and maximum respiration were determined (Fig. 2B). In vehicle-control cells, the bioenergetics profile demonstrated the expected response pattern for basal respiration and following each inhibitor. Basal respiration was significantly increased following exposure to PBP (10 μM, $p<0.0001$) and decreased at 40 μM ($p=0.01$), as compared to controls. No significant differences were observed for TBBPA or TPP, although a higher level of variance was observed for 40 μM TBBPA with individual samples showing levels to those observed with PBP. ATP-linked respiration was significantly decreased with 40 μM PBP ($p<0.0001$) and TBBPA ($p<0.001$) suggesting an alteration in electron transport in a manner that affects ATP production. No differences were observed with 10μM PBP, TBBPA, or either dose of TPP. Maximum respiration was significantly altered by exposure to all FR ($p<0.01$). Exposure to PBP showed an increase in maximum respiration at 10 μM ($p<0.01$) and a decrease at 40 μM ($p<0.0001$) consistent with the other endpoints. Exposure to TBBPA showed a significant increase at 10 μM ($p<0.01$) and decrease at 40 μM ($p<0.001$). A significant increase was observed for TPP at both dose levels ($p<0.001$; 0.01, respectively).

In microglia, cellular metabolism and pro-inflammatory response can be affected by altered glycolytic rate (Orihuela et al. 2016). The Seahorse Bioanalyzer was used to measure proton efflux rate (PER) and extracellular acidification as surrogates for glycolysis. This data was collected in the absence (for basal) or presence of rotenone, a mitochondrial complex I inhibitor, and 2-deoxyglucose (2-DG) to inhibit glycolysis and provide information on the ability of cells to compensate for electron transport chain inhibition by increasing their glycolytic rate (Fig. 2C). In controls, a normal pattern of increased glycolysis was observed with rotenone (calculated as compensatory glycolysis), which was blocked by addition of 2-DG. The mean basal glycolytic rate (Fig. 2D) was increased by exposure to PBP (10 μM, $p=0.0125$; 40 μM, $p<0.0001$). For TBBPA, no changes were observed at 10μM but a significant increase was observed at 40 μM ($p=0.0003$). The absence of additional stimulation by rotenone suggested a maximized glycolytic capacity. No significant differences in basal glycolytic rate were observed for TPP. A significant decrease in compensatory glycolysis (Fig. 2D) was observed at the 40 μM dose level for PBP ($p=0.0002$) and TBBPA ($p=0.0003$) with no differences observed at the lower dose level. Both dose levels of TPP showed a significant decrease in compensatory glycolysis ($p=0.029$; $p<0.0002$, respectively) as compared to controls.

These findings suggested that these compounds differentially affect microglia metabolism via mitochondrial oxidative phosphorylation or glycolysis but not necessarily both. To support this interpretation of cellular processes, the rho+ and rho0 isogenic 143B osteosarcoma cell lines were examined following FR exposure. These cells either contain (rho+) and thus generate ATP both by mitochondrial OXPHOS and glycolysis or are depleted of mitochondrial DNA (mtDNA; rho0) and can only produce ATP through glycolysis due to a lack of functional OXPHOS (Lozoya et al., 2019). Following exposure to each FR, dose levels ≥25μM showed a progressive decrease in ATP levels in both rho+ (Fig. 3A) and rho0 cells (Fig. 3B) that was related to the loss of cells. A comparison across the cell lines showed a general increase in ATP levels at doses ≤12.5μM in the absence of decreased cell number. The dependency of rho0 cells on glycolysis and the effects of the test

compounds were evident in the dose-response changes in ATP levels at dose levels <25μM suggesting changes in glycolytic rate, consistent with findings in the BV-2 cells.

3.4 qRT-PCR for *Tnfa, Il1a,* and *Ccl3*

In macrophages, increased aerobic glycolysis has been associated with elevations in the proinflammatory cytokine response and alterations in metabolism can influence response to an inflammatory challenge. mRNA levels for *Tnfa, Il1a, and* chemokine ligand 3 (macrophage inflammatory protein 1-alpha), *Ccl3* were examined following 18 hr exposure to FRs (Fig. 4). For PBP, *Tnfa* levels were significantly different ($F_{(2,15)}$=11.29, p=0.001) with a statistically significant decrease seen at 40 μM as compared to control (p=0.015). *Il1a* was significantly different ($F_{(2,15)}$=9.159, p=0.003) with a statistically significant decrease seen at 40 μM as compared to control (p=0.013). For TBBPA, *Tnfa* levels were significantly altered ($F_{(2,15)}$=6.039, p=0.012) with a statistically significant elevation seen at 40 μM as compared to control (p=0.007). *Il1a* levels were not significantly changed. Data obtained from TPP exposure failed to meet homogeneity of variance by Brown-Forsythe or Bartlett's test thus, a Kruskal-Wallis test was used for analysis. *Tnfa* levels were not significantly altered while *Il1a* levels were significantly altered (7.626, p=0.015) with levels significantly lower in the 10 μM dose group as compared to controls (p=0.014). In the 40 μM dose level, a dichotomy of response was observed across samples. In all dose groups, levels of chemokine ligand 3 (macrophage inflammatory protein 1-alpha), *Ccl3* were not altered by exposure.

3.5 TNFα and IL-1 protein levels

For PBP exposure, TNF protein levels were significantly lower at 40 μM (p<0.05) as compared to controls. Levels following TBBPA exposure were slightly increased however, this failed to reach statistical significance. No changes were observed for TPP (Fig. 5A). IL-1 (IL-1α and IL-1β) released into the cell medium was detected by HEK-Blue IL-1R reporter cells. In general, this assay is limited in its ability to provide a quantitative measure of IL-1 but rather can be used as an indicator of protein presence. An increase in reporter indicator suggested the release of IL-1 from BV-2 cells exposed to 10 μM PBP (p<0.05) (Fig. 5B). The reporter indication was similar to controls for all other groups.

3.6 mRNA changes following LPS challenge

To determine if exposure to these FRs at 10 μM would alter microglia response to a pro-inflammatory stimulus, cells exposed to FRs for 18 hr were challenged by the addition of LPS. Under these conditions, the prior exposure to the FRs did not significantly alter the ability of the cells to respond to the LPS challenge (Fig. 6).

3.7 Phagocytosis

One of the primary functions of microglia, as for other macrophage-type cells, is the ability to phagocytize and clear aberrant material from the tissue. This shift to a phagocytic phenotype places an energy demand on the cells and thus, changes in mitochondria can likely impact such functional actions of microglia. To determine if alterations in phagocytic function were induced, the engulfment of bacterial fragments of various concentrations was examined in cells exposed to the FRs at the 10 μM dose level (Fig. 7). With the

addition of bacterial fragments (10, 25, or 50 μg/mL) all cells showed the ability to engulf the material and an increase was observed between 10 μg/mL and 25 μg/mL fragment concentrations ($p<0.001$). No additional phagocytic capacity was observed with an increase in fragment concentration to 50 μg/mL. When the phagocytic response was analyzed at each of the fragment concentrations, no significant differences were noted at the 10 μg/mL concentration. When the fragment concentration was increased to 25 μg/mL, a significantly lower level of uptake was observed for PBP ($p<0.01$) and TBBPA ($p<0.05$). At the 50 μg/mL concentration, a lower level of phagocytosis was observed for PBP ($p<0.05$). No change in phagocytosis was observed with TPP.

3.8 NLRP3 Inflammasome Activation

One mechanism by which the inflammatory response is initiated and possibly regulated is through inflammasome activation. Of the different inflammasomes, the NLRP3 inflammasome can be triggered by sterile factors thus, potentially representing a site of action for environmental compounds to influence the inflammatory response. In immune cells primed following toll like receptor activation, a secondary-stimuli can serve as a trigger to activate the NLRP3 inflammasome. With activation, NLRP recruits ASC and the cysteine protease caspase 1 forming an ASC speck protein aggregate that promotes the activation of caspase-1 for the release of mature IL-1β. Mitochondria function is associated with NLRP3 inflammasome activation. Given the subtle alterations observed in mitochondria, the FRs were examined to determine if they can serve as a secondary trigger. Inflammasome activation was assessed using BV-2-ASC cells to visualize ASC speck formation as an indicator of inflammasome activation. As an indicator of individual cell responses, the formation of ASC-specks was identified by live-cell imaging. Under control conditions and with LPS-priming, a diffuse cytoplasmic staining was observed with no evidence of ASC-speck formation (Fig. 8). A similar diffuse staining was observed in non-primed cells with TBBPA and TPP while, PBP significantly increased aggregate number (116.2 +/−11.16; t=4.569, df=9; p<0.0013) suggestive of a non-canonical activation. In the positive control for NLRP3 inflammasome activation, the addition of ATP to LPS-primed cells induced pronounced speck aggregate formation (Fig. 8). When the potential for each of the FRs to serve as a secondary trigger in LPS-primed cells was examined, PBP showed a significant increase in ASC speck formation as compared to vehicle control ($p<0.0018$) and as compared to non-LPS primed cells exposed to PBP ($p<0.0043$). LPS+TBBPA showed evidence of aggregate formation that failed to reach statistical significance and, with LPS+TPP, the diffuse staining pattern was maintained with no evidence of aggregate formation. Corresponding cell morphology as demonstrated in phase-contrast images indicated subtle differences in LPS-primed cells exposed to FRs (Fig. 8). The normal morphological pattern of rounded and triangular flattened was observed in LPS-primed cells exposed to ATP or TPP. For PBP, the cells primarily maintained a rounded morphology with the inclusion of a small proportion of rodlike cells. For TBBPA, cells showed a primary rounded morphology with little evidence of triangle or elongated morphology.

4. DISCUSSION

Microglia play critical roles in defining the structure and function of the nervous system. Alterations in the ability of microglia to perform such functions or a shift in the threshold for the cells to respond can have significant adverse effects across a diverse array of processes. Based upon previous reports suggesting effects of TBBPA on immune cells, the current study examined various aspects of microglia response to specific FR exposure using the BV-2 cell line. At dose levels producing little if any changes in cell viability, comparisons were made among BFRs (i.e., PBP and TBBPA) and the OPFR FR, TPP. The predominant effect observed was in the examination of mitochondrial bioenergetics with PBP showing the greatest level of alterations however, maximum respiration and compensatory glycolysis were affected by all 3 FRs. The changes in mitochondria observed with PBP were accompanied by a direct triggering of ASC-speck aggregation and, at the higher 40 μM concentration, PBP exposure decreased levels of *Tnfa* and *Il1a* but did not alter LPS-induced elevation. TBBPA elevated *Tnfa* levels and with TPP, *Il1a* was decreased at the lower dose level. Shifts in cellular metabolism serve as determinants of macrophage function and phenotype (Artyomov et al., 2016) and changes in microglia metabolism may alter their ability to respond to various signals from the environment.

Associated functional changes were observed for PBP and TBBPA for phagocytosis while the cells maintained the ability to respond to an LPS challenge. PBP clearly demonstrated the ability to function as an secondary trigger for NLRP3 inflammasome activation with suggestions of similar properties for TBBPA. Overall, the effects of TPP exposure were minimal suggesting that any observed change in mitochondrial respiration is related to a cell survival process given the lower level of cell viability starting to be observed with increasing dose levels of this FR.

During mito-energetic dysfunction, the cell's ability to alter the balance between glycolytic and mitochondrial ATP generation is crucial for survival (Bonora et al., 2012). In the cytosol, ATP can be produced by glycolytic conversion of glucose into pyruvate which can be metabolized into lactate. This is released by the cell or taken up by mitochondria to fuel ATP production by the tricarboxylic acid cycle and oxidative phosphorylation and thus, can compensate for the loss in mitochondrial ATP production (Liemburg-Apers et al., 2015). Kibakaya et al. (2009) reported decreased intracellular ATP levels in NK cells exposed for 24 hr to TBBPA at dose levels as low as 5μM. In the current study, we observed a similar decrease in ATP levels in the rho cells consistent with the effects on ATP metabolism observed in the BV-2 cells. Lower respiration responses and oxidative phosphorylation levels observed at 40μM TBBPA were associated with an increase in basal glycolytic rate, with no alterations observed at the lower 10 μM dose level. Given the absence of cell death, it is likely that this process was utilized for cellular survival. In comparison, PBP initiated an increase in both anaerobic and aerobic metabolism, suggestive of cells with functioning mitochondria. At the higher dose level, the lower level of mitochondrial respiration, accompanied by an elevation in basal glycolytic rate, also likely represented a survival mechanism, similar to TBBPA. Very little reported data is available for TPP but the absence of alterations in ATP-linked respiration yet changes in maximum respiration suggest mitochondrial-independent oxygen consumption possibly

as an alternative adaptation response preceding overt toxicity. One possibility for the contrasting mitochondrial profiles generated with PBP or TBBPA as compared to TPP may be related to a difference in P450 enzyme activation. It has been previously reported that P450 enzymes can actively metabolize TPP (Screening Information Data Set (SIDS), 2006) and it is known that, with the pro-inflammatory stimulus, interferon-gamma, BV-2 cells can elevate various P450 isoforms (Snider et al., 2009). It is likely that the increased maximum respiration observed is associated with activation of P450 oxygenases to catalyze the incorporation of oxygen atoms from molecular oxygen into their organic substrates. While these are speculated effects, they would be consistent with observations on the metabolic profile of mice exposed to TPP during the early postnatal period suggesting shifts in lipid-related metabolites at low-exposure levels and a down-regulation of pyruvate metabolism and TCA cycle with the higher levels of 200 μg/day (Wang et al. 2018).

Mitochondria play a crucial role in the inflammatory signaling of immune cells (Mills et al., 2016) and BV-2 cells show increased aerobic glycolysis with a pro-inflammatory response to LPS (Orihuela et al., 2016). Previous work reported immune cell-specific decreases in IL-1β secretion following exposure to TBBPA at dose levels >5μM (Anisuzzaman and Wallen, 2016). In the current study, few changes in pro-inflammatory cytokine levels were observed at the 10 μM dose level. With the higher level, 40 μM, a decrease was observed with PBP and an elevation with TBBPA. TPP was not without effect in that lower expression levels were also observed. These subtle changes did not lead to a deficit in the ability of BV-2 cells to respond to an LPS challenge. When the findings were compared to a similar experimental study examining the effects of TBBPA on RAW 264.7 cells (Wang et al., 2019) an elevation in *Tnfa* was observed. Functionally, Wang et al (2019) reported that RAW 264.7 cells exposed to TBBPA could demonstrate a response to LPS however, this response was attenuated by approximately 30%. Similarly, we report that BV-2 cells exposed to FRs could respond to LPS however, a significant attenuation was not observed. The difference between the studies may be related to the cell type but also differences in time of exposure as well as time and dose for LPS stimulation. When the functional change in immune-cell phagocytosis was compared between the two studies a decrease in phagocytosis was observed for TBBPA in both BV-2 and RAW 264.7 cells. Data obtained from the two studies suggest that exposure to TBBPA alters the functional response of macrophage-like cells that may be associated with changes in the bioenergetics of the cells.

To further examine the ability of FRs to influence the inflammatory response, we examined the ability the FRs to function as a secondary stimulus for inflammatory activation. Within the inflammatory repertoire, inflammasome activation plays an ever-increasing role for which a contributory role of mitochondrial function has been implicated (for review, Gurung et al., 2015; Elliott et al., 2018). Inflammasomes are multiprotein complexes that form in the cytosol of immune and neural cells in response to danger signals. Upon activation they elicit or lower an inflammatory response threshold and can inform the subsequent adaptive immune response (Broz and Dixit, 2016; Evavold and Kagan 2018; Latz 2010). The NLRP inflammasome recognizes a range of microbes and sterile danger signals and thus, can contribute to a broad range of common inflammatory pathologies (Gross et al., 2011). In n cells, NLRP3 is diffuse in the cytosol. Activation is induced by a variety of endogenous triggers including damaged mitochondria and ROS (Zhou et al., 2011) and,

upon activation, NLRP3 translocates to the mitochondrial membrane (Elliott et al., 2018; Zhou et al., 2011). For PBP, in addition to the canonical activation observed in LPS-primed cells, the formation of ASC specks in non-primed cells suggested a non-canonical activation of the NLRP3 inflammasome which could be associated with the altered mitochondrial respiration observed. A slight increase in ASC-speck production was observed with TBBPA in LPS-primed cells; however, at the short 6 hr time interval, this was not statistically significant. In comparison, TPP did not appear to function as a secondary trigger or to induce a non-canonical activation. NLRP3 inflammasome activation results in the release of mature IL-1β and has been associated with pyroptosis and the transition of an acute inflammatory response to a more prolonged chronic inflammation. When the resulting ASC specks are released into the extracellular environment they can contribute to a number of biological responses in the nervous system and may significantly contribute to a prolonged inflammatory response (Venegas et al., 2017). Thus, products released as a result of inflammasome activation, IL-1β and ASC specks, can represent neurotoxic signaling and the potential for adverse effects on the nervous system.

While the current study demonstrates the ability of these FRs to act upon cultured microglia cells, how this might translate to potential effects in the nervous system remains to be determined. A recent review by Kacew and Hayes (2020) suggested that, in the absence of data demonstrating entry of TBBPA into the brain parenchyma and the lack of neuropathology, data suggestive of a classification of neurotoxic is not well founded. While this is a sound argument for deliberation, there are other considerations. First of all, there is a paucity of analytical data on the amount of flame retardants that actually reach the brain. In fact, there are few distribution studies that take into consideration the significant contribution of the blood compartment within the brain and remove the blood prior to tissue collection. While target tissue levels are critically important in any assessment of neurotoxicity, excluding consideration of neurotoxicity simply due to an absence of confirmation of chemical levels at peak time following exposure or persistence may not be prudent. The second point relates to the recent publication demonstrating an effect of TBBPA on the ABC blood-brain-barrier (BBB) transporter (Cannon et al., 2019). While a change in transporter does not necessarily represent a “neurotoxic” effect, as pointed out by Kacew and Hayes (2020), such shifts may have an effect upon cells in intimate contact such as, astrocytes and microglia. Another critical consideration for neurotoxicity in the absence of direct chemical entry into the target tissue, is the influence of hormones on brain development and functioning. Of relevance to the current study, thyroid hormones regulate activities of key enzymes of glycolysis, affecting macrophage metabolism and function (Curi et al., 2017). *In vivo* exposure to TBBPA has been reported to induce hypothyroxinemia (Cope et al., 2015; NTP, 2014) possible through competition with the thyroid hormone receptor for binding to transthyretin (review, Colnot et al., 2014). An interplay between thyroid hormone action and peripheral immune cells has been established with evidence of actions in both the innate and adaptive immune responses (Montesinos and Pellizas, 2019). Earlier work reported that microglia express the a1 and b1 isoforms of nuclear thyroid hormone receptors (Lima et al., 2001) and, under conditions of developmental hypothyroxinemia, show a decrease in cellprocess complexity (Harry et al., 2014; Lima et al., 2001) and diminished response to a LPS challenge (Opazo et al., 2018). Thus, if

exposure results in a direct effect upon microglia or if the effect is secondary to a shift in thyroid hormone or a change in BBB transporters, there remains an effect upon these critical cells of the brain even if only localized to those microglia in contact with the vascular wall.

In summary, the present study suggested that the various effects observed with the BFRs, PBP and TBBPA, and with the alternative, OPFR, TPP, may be related to altered mitochondrial bioenergetics. This possible relationship warrants further examination to determine exactly what this cellular response to exposure represents with regards to biological function and how such changes might reflect a shift in reserve capacity and possibly manifest as a future adverse health effect.

Acknowledgements:

Christine Bowen, Gabrielle Childers, and Caroline Perry conducted much of the experiments and were involved in the conceptualization of the study, Dr. Negin Martin designed and generated the BV2 ASC speck cells; Dr. Janine Santos established the cell-based assays for mitochondrial screening, Dr. G. Jean Harry contributed to the conceptualization and interpretation of the study and supervision of the experiments. Tatlock Lauten provided technical validation of the mRNA data and Dr. Christopher McPherson provided expertise for image and data analysis. All authors contributed to writing of the final manuscript. The authors wish to acknowledge the expert assistance of Dr. Guan Xie, Social & Scientific Systems, Durham, NC, for statistical analysis and Lois Wyrick for graphics. Drs. Will Gwinn and Kristen Ryan provided reviewer comments on the manuscript. The research was supported by NIH intramural research funding Z01 ES021164–12; and statistical consulting contract HHSN273201600011C.

REFERENCES

Aarum J, Sandberg K, Haeberlein SL, et al.2004. Migration and differentation of neural precursor cells can be directed by microglia. Proc. Natl. Acad. Sci. USA100:15983–15988.

Abou-Donia MB, Salama M, Elgamal M. et al.2016. Organophosphorus Flame Retardants (OPFR): Neurotoxicity. J. Environ. Health Sci. doi.10.15436/2378-6841.16.022

Alam TM, Neerathilingam M, Alam MKet al.2012. 1H Nuclear Magnetic Resonance (NMR) Metabolomic Study of Chronic Organophosphate Exposure in Rats. Metabolites2(3):479–495. doi: 10.3390/metabo2030479. [PubMed: 24957643]

Al-Mousa F, Michelangeli F. 2012. Some commonly used brominated flame retardants cause Ca2+-ATPase inhibition, beta-amyloid peptide release and apoptosis in SH-SY5Yneuronal cells. PLOS ONE. 7(4):e33059.10.1371/journal.pone.0033059

Anisuzzaman S, Whalen MM2016. Tetrabromobisphenol A and hexabromocyclododecane alter secretion of Il-1β from human immune cells. J. Immunotoxicol. 13:403–416. [PubMed: 27297965]

Arita Y, Pressman M, Getahun D, et al.2018. Effect of Tetrabromobisphenol Aon expression of biomarkers for inflammation and neurodevelopment by the placenta. Placenta. 68:33–39. [PubMed: 30055667]

Artyomov MN, Sergushichev A, Schilling JD2016. Integrating immunometabolism and macrophage diversity. Semin. Immunol. 28:417–424. [PubMed: 27771140]

Behl M, Hsieh J-H, Shafer TJ, et al.2015. Use of alternative assays to identify and prioritize organophosphorus flame retardants for potential developmental and neurotoxicity. Neurotoxicol. Teratol. 52:181–193. [PubMed: 26386178]

Birnbaum LS, Staskal DF2004. Brominated flame retardants: Cause for concern?. Environ. Hlth. Persp. 112: 9–17.

Bonora M, Patergnani S, Rimessi A, et al.2012. ATP synthesis and storage. Purinergic Signal8:343–357. [PubMed: 22528680]

Brawek B, Liang Y, Savitska D, et al.2017. A new approach for ratiometric in vivo calcium imaging of microglia. Sci. Rep. 7:6230. [PubMed: 28740086]

Broz P, Dixit VM. 2016. Inflammasomes: mechanism of assembly, regulation and signalling. Nat Rev Immunol16(7):407–20. doi:10.1038/nri.2016.58 [PubMed: 27291964]

Cannon RE, Trexler AW, Knudsen GA, et al.2019. Tetrabromobisphenol A (TBBPA) alters ABC transport at the blood-brain barrier. Toxicol. Sci. 169:475–484. [PubMed: 30830211]

Cariou R, Antignac J-P, Zalko D, et al.2008. Exposure assessment of French women and their newborns to Tetrabromobisphenol-A: Occurrence measurements in maternal adipose tissue, serum, breast milk and cord serum. Chemosphere73:1036–1041. [PubMed: 18790516]

Castorina R, Bradman A, Stapleton HM, et al.2017. Current-Use Flame Retardants: Maternal Exposure and Neurodevelopment in Children of the CHAMACOS cohort. Chemosphere189:574–580. [PubMed: 28963974]

Cato A, Celada L, Kibakaya EC, et al.2014. Brominated flame retardants, tetrabromobisphenol A and hexabromocyclododecane, activate mitogen-activated protein kinases (MAPKs) in human natural killer cells. Cell. Biol. Toxicol. 30:345–360. [PubMed: 25341744]

Chen G, Jin Y, Wu Y, et al.2015. Exposure of male mice to two kinds of organophosphate flame retardants (OPFRS) induced oxidative stress and endocrine disruption. Environ. Toxicol. Pharmacol. 40:310–318. [PubMed: 26183808]

Colnot T, Kacew S, Dekant WJ2014. Mammalian toxicology and human exposures to the flame retardant 2,2′,6,6′-tetrabromo-4,4′-isopropylidenediphenol (TBBPA): Implications for risk assessment. Arch. Toxicol. 88(3):553–573. [PubMed: 24352537]

Cope R, Kacew S, Dourson M. 2015. A reproductive, developmental and neurobehavioral study following oral exposure of Tetrabromobisphenol A on Sprague-Dawley rats. Toxicol. 329:49–59.

Curi R, de Siqueira Mendes R, de Campos Crispin LA, et al.2017. A past and present overview of macrophage metabolism and functional outcomes. Clin. Sci. 131:1329–1342.

De Wit M, Keil D, Remmerie N, et al.2008. Molecular targets of TBBPA in zebrafish analysed through integration of genomic and proteomic approaches. Chemosphere74:96–105. [PubMed: 18976794]

Diamandakis D, Zieminska E, Siwiec M,, et al.2019. Tetrabromobisphenol A-induced depolarization of rat cerebellar granule cells: ex vivo and in vitro studies. Chemosphere223:64–73. [PubMed: 30769291]

Dietert RR2015. Effects of endocrine disrupters on immune function and inflammation. In: (Ed: Darbre PD). Endocrine disruption and human health. Boston: Academic Press p. 257–272.

Dingemans MML, van den Berg M, Westerink RHS2011. Neurotoxicity of brominated flame retardants: (In)direct effects of parent and hydroxylated polybrominated diphenyl ethers on the (Developing) nervous system. Environ. Hlth. Persp. 119:900–907.

Du Z, Wang G, Gao S, et al.2015. Aryl organophosphate flame retardants induced cardiotoxicity during zebrafish embryogenesis: by disturbing expression of the transcriptional regulators. Aquat. Toxicol. 161:25–32. [PubMed: 25661707]

Du Z, Zhang Y, Wang G, et al.2016. TPhP exposure disturbs carbohydrate metabolism, lipid metabolism, and the DNA damage repair system in zebrafish liver. Sci. Rep. 22;6:21827. doi: 10.1038/srep21827

Elliott EI, Miller AN, Banoth B, et al.2018. Cutting Edge: Mitochondrial Assembly of the NLRP3 Inflammasome Complex Is Initiated at Priming. J. Immunol. 200:3047–3052. [PubMed: 29602772]

Erblich B, Zhu L, Etgen AM, et al.2011. Absence of colony stimulation factor-1 receptor results in loss of microglia, disrupted brain development and olfactory deficits. PLOS ONE6(10):e26317.10.1371/journal.pone.0026317

Eriksson P, Vberg H. 2011. Differences in neonatal neurotoxicity of brominated flame retardants, PBDE 99 and TBBPA, in mice. Toxicology289:59–65. [PubMed: 21820030]

(ECB) European Union Risk Assessment Report (2006) 2,2’,6,6’-tetrabromo-4,4’-isopropylidenediphenol (tetrabromobisphenol-A or TBBP-A) (CAS: 79–94–7) Part II – human health. Institute for Health and Consumer Protection, European Chemicals Bureau, European Commission Joint Research Centre, 4th Priority List, Luxembourg: Office for Official Publications of the European Communities.

Gross O,, Thomas CJ, Guarda G,, et al.2011. The inflammasome: an integrated view. Immunol. Rev. 243:136–151. [PubMed: 21884173]

Evavold CL, Kagan JC2018. How Inflammasomes Inform Adaptive Immunity. J. Mol. Biol. 430:217–237. [PubMed: 28987733]

Gurung P, Lukens JR, Kanneganti T-D2015. Mitochondria: Diversity in the regulation of NLRP3 inflammasome. Trends Mol. Med. 21:193–201. [PubMed: 25500014]

Hall SM, Coulter SJ, Knudsen GA, et al.2017. Gene expression changes in immune response pathways following oral administration of Tetrabromobisphenol A (TBBPA) in female Wistar Han rats. Toxicol. Lett. 272:68–74. [PubMed: 28300664]

Han EH, Park JH, Kang KW, et al.2009. Risk assessment of Tetrabromobisphenol A on cyclooxygenase-2 expression via MAP kinase/NF-κB/AP-1 signaling pathways in murine macrophages. J. Toxicol. Environ. Health Part A72(21–22):1431–1438.

Harry GJ, Kraft AD2012. Microglia in the developing brain: A potential target with lifetime effects. Neurotoxicology33:191–206. [PubMed: 22322212]

Harry GJ, Pont-Lezica L. 2014. Developmental vascularization, neurogenesis, myelination, and astrogliogenesis. In: Tremblay M-È, Sierra A, editors. Microglia in health and disease. New York, NY: Springer New York. p. 193–221.

Harry GJ, Hooth MJ, Vallant M, et al.2014. Developmental neurotoxicity of 3,3',4,4'-tetrachloroazobenzene with thyroxine deficit: Sensitivity of glia and dentate granule neurons in the absence of behavioral changes. Toxics2:496–532. [PubMed: 26029700]

Hendriks HS, Westerink RH2015. Neurotoxicity and risk assessment of brominated and alternative flame retardants. Neurotox. Terat. 52:248–269.

Hendriks HS, van Kleef RG, van den Berg M, et al.2012. Multiple novel modes of action involved in the in vitro neurotoxic effects of Tetrabromobisphenol-A. Toxicol. Sci. 128:235–246. [PubMed: 22547355]

Hommel G. 1988. A stagewise rejective multiple test procedure based on a modified Bonferroni test. Biometrika. 75:383–386.

Isales GM, Hipszer RA, Raftery TD, et al.2015. Triphenyl phosphate-induced developmental toxicity in zebrafish: potential role of the retinoic acid receptor. Aquat. Toxicol. 161:221–30. [PubMed: 25725299]

Hughes MM, O'Neill LAJ2018. Metabolic regulation of NLRP3. Immunol. Rev. 281:88–98. [PubMed: 29247992]

Kacew S, Hayes AW2020. Absence of neurotoxicity and lack of neurobehavioral consequences due to exposure to tetrabromobisphenol A (TBBPA) exposure in humans, animals and zebrafish. Arch. Toxicol. 94:59–66. [PubMed: 31758204]

Kibakaya EC, Stephen K, Whalen MM2009. Tetrabromobisphenol A has immunosuppressive effects on human natural killer cells. J. Immunotoxicol. 6:285–292. [PubMed: 19908946]

Kim AH, Chun HJ, Lee S, et al.2017. High dose tetrabromobisphenol A impairs hippocampal neurogenesis and memory retention. Food Chem. Toxicol. 106(Pt A):223–231. [PubMed: 28564613]

Lee S, Lee H, Kim KT2019. Optimization of experimental conditions and measurement of oxygen consumption rate (OCR) in zebrafish embryos exposed to organophosphate flame retardants (OPFRs). Ecotoxicol. Environ. Saf. 182:109377. doi: 10.1016/j.ecoenv.2019.109377.

Lenart J, Zieminska E, Diamandakis D, Lazarewicz JW. 2017. Altered expression of genes involved in programmed cell death in primary cultured rat cerebellar granule cells acutely challenged with tetrabromobisphenol A. Neurotoxicology63:126–136. [PubMed: 28970181]

Lewis RJ Sr.2004. Sax's Dangerous Properties of Industrial Materials. 11th Edition. Wiley-Interscience, Wiley &Sons, Inc. Hoboken, NJ.

Liang S, Liang S, Zhou H, et al.2019. Typical halogenated flame retardants affect human neural stem cell gene expression during proliferation and differentiation via lycogen synthase kinase 3 beta and T3 signaling. Exotoxicol. Environ. Safety183:109498. doi.10.1016/j.ecoenv.2019.109498

Liemburg-Apers DC, Schirris TJ, Russel FG, et al.2015. Mitoenergetic Dysfunction Triggers a Rapid Compensatory Increase in Steady-State Glucose Flux. 109:1372–1386.

Lima RF, Gervais A, Colin C, et al.2001. Regulation of microglia development: a novel role for thyroid hormone. J. Neurosci. 21:2028–2038. [PubMed: 11245686]

Liu X, Cai Y, Wang Y, Xu S, Ji K, Choi K. 2019. Effects of tris(1,3-dichloro-2-propyl) phosphate (TDCPP) and triphenyl phosphate (TPP) on sex-dependent alterations of thyroid hormones in adult zebrafish. Ecotoxicol Environ Saf. 170:25–32. [PubMed: 30508752]

Lozoya OA, Martinez-Reyes I, Wang T, Grenet D, Bushel P, Li J, Chandel N, Woychik RP, Santos JH. 2018. Mitochondrial nicotinamide adenine dinucleotide reduced (NADH) oxidation links the tricarboxylic acid (TCA) cycle with methionine metabolism and nuclear DNA methylation. PLoS Biol16(4):e2005707. doi: 10.1371/journal.pbio.2005707

Mäkinen MS, Mäkinen MR, Koistinen JT, et al.2009. Respiratory and dermal exposure to organophosphorus flame retardants and tetrabromobisphenol A at five work environments. Environ. Sci. Technol. 43:941–947. [PubMed: 19245040]

Malliari E, Kalantzi OI2017. Children's exposure to brominated flame retardants in indoor environments - A review. Environ. Int. 108:146–169. [PubMed: 28863388]

McGee SP, Konstantinov A, Stapleton HM, et al.2013. Aryl phosphate esters within a major PentaBDE replacement product induce cardiotoxicity in developing zebrafish embryos: potential role of the aryl hydrocarbon receptor. Toxicol. Sci. 133:144–156. [PubMed: 23377616]

Meeker JD, Cooper EM, Stapleton HM, et al.2013. Urinary metabolites of organophosphate flame retardants: Temporal variability and correlations with house dust concentrations. Environ. Hlth. Persp. 121:580–585.

Mills EL, Kelly B, O'Neill LAJ2017. Mitochondria are the powerhouses of immunity. Nat. Immunol. 18(5):488–498. [PubMed: 28418387]

Mitchell CA, Dasgupta S, Zhang S, et al.2018. Disruption of Nuclear Receptor Signaling Alters Triphenyl Phosphate-Induced Cardiotoxicity in Zebrafish Embryos. Toxicol. Sci. 163(1):307–318. [PubMed: 29529285]

Montesinos MDM, Pellizas CG2019. Thyroid hormone action on innate immunity. Front. Endocrinol. (Lausanne). 64;10:350. doi: 10.3389/fendo.2019.00350. [PubMed: 31214123]

Nakajima A, Saigusa D, Tetsu N, et al.2009. Neurobehavioral effects of tetrabromobisphenol A, a brominated flame retardant, in mice. Toxicol. Lett.189:78–83. [PubMed: 19463927]

National Toxicology Program, National Institutes of Health RTP, NC. 2014. Technical report on the toxicology studies of tetrabromobisphenol a (cas no. 79–94–7) in F344/ntac rats and b6c3f1/n mice and toxicology and carcinogenesis study of tetrabromobisphenol a in wistar han rats and B6C3f1/n mice (gavage studies). Accessed 4/14/2020. https://ntp.niehs.nih.gov/ntp/htdocs/lt_rpts/tr587_508.pdf?utm_source=direct&utm_medium=prod&utm_campaign=ntpgolinks&utm_term=tr587.

Noda M. 2018. Thyroid Hormone in the CNS: Contribution of Neuron-Glia Interaction. Vitam. Horm. 106:313–331. [PubMed: 29407440]

Latz E. 2010. NOX-free inflammasome activation. Blood. 116:1393–1394. [PubMed: 20813905]

Opazo MC, Gnzalez PA, Flores BD, et al.2018. Gestational hypothyroxinemia imprints a switch in the capacity of astrocytes and microglial cells of the offspring to react in inflammation. Mol. Neurobiol. 55:4373–4387. [PubMed: 28656482]

Orihuela R, McPherson CA, Harry GJ2016. Microglial m1/m2 polarization and metabolic states. Br. J. Pharmacol. 173(4):649–665. [PubMed: 25800044]

Orsi NM, Tribe RM. 2008. Cytokine networks and the regulation of uterine function in pregnancy and parturition. J Neuroendocrinol20(4):462–469. [PubMed: 18266939]

Park H-R, Kamau PW, Korte C, Loch-Caruso RJ. 2014. Tetrabromobisphenol A activates inflammatory pathways in human first trimester extravillous trophoblasts in vitro. Reprod Toxicol50:154–162. [PubMed: 25461914]

Park SY, Choi EM, Suh KS, et al.2019. Tetrabromobisphenol A Promotes the Osteoclastogenesis of RAW264.7 Cells Induced by Receptor Activator of NF-kappa B Ligand In Vitro. J. Korean Med. Sci. 34(4) doi.10.3346/jkms.2019.34.e267

Próchnicki T, Latz E. 2017. Inflammasomes on the Crossroads of Innate Immune Recognition and Metabolic Control. Cell Metab. 26(1):71–93. [PubMed: 28683296]

Phillips AL, Hammel SC, Hoffman K, et al.2018. Children's residential exposure to organophosphate ester flame retardants and plasticizers: Investigating exposure pathways in the TESIE study. Environ. Int. 116:176–185. [PubMed: 29689464]

Reistad T, Mariussen E, Fonnum F. 2005. The effect of a brominated flame retardant, Tetrabromobisphenol-A, on free radical formation in human neutrophil granulocytes: the

involvement of the MAP kinase pathway and protein kinase C. Toxicol. Sci. 83:89–100. [PubMed: 15456914]

Reistad T, Mariussen E, Ring A, et al.2007. In vitro toxicity of tetrabromobisphenol-a on cerebellar granule cells: Cell death, free radical formation, calcium influx and extracellular glutamate. Toxicol. Sci. 96:268–278. [PubMed: 17205976]

Saegusa Y, Fujimoto H, Woo GH, et al.2012. Transient aberration of neuronal development in the hippocampal dentate gyrus after developmental exposure to brominated flame retardants in rats. Arch. Toxicol. 86:1431–42. [PubMed: 22415764]

Salmon P, Trono D. 2006. Production and titration of lentiviral vectors. Curr. Prot. Neurosci. 37(1) doi.10.1002/0471142301.ns0421s37

Schafer DP, Lehrman EK, Kautzman AG, et al.2012. Microglia sculpt postnatal neural circuits in an activity and complement-dependent manner. Neuron74:691–705. [PubMed: 22632727]

Schauer UMD, Völkel W, Dekant W. 2006. Toxicokinetics of Tetrabromobisphenol A in Humans and Rats after Oral Administration. Toxicol. Sci, 91:49–58, [PubMed: 16481339]

Schindelin J, Arganda-Carreras I, Frise E, et al.2012. Fiji: An open-source platform for biological-image analysis. Nat. Methods9(7):676. [PubMed: 22743772]

Shi Q, Tsui MMP, Hu C, et al.2019. Acute exposure to triphenyl phosphate (TPhP) disturbs ocular development and muscular organization in zebrafish larvae. Ecotoxicol. Environ. Saf. 179:119–126. [PubMed: 31035246]

Shi Q, Wang M, Shi F, et al.2018. Developmental neurotoxicity of triphenyl phosphate in zebrafish larvae. Aquat. Toxicol. 203:80–87. [PubMed: 30096480]

Shi Y, Zheng X, Yan X, et al.2019. Short-term variability in levels of urinary phosphate flame retardant metabolites in adults and children from an e-waste recycling site. Chemosphere234:395–401. [PubMed: 31228842]

Shi ZX, Wu YN, Li JG, et al.2009. Dietary exposure assessment of chinese adults and nursing infants to tetrabromobisphenol-A and hexabromocyclododecanes: occurrence measurements in foods and human milk. Environ. Sci. Technol. 3:4314–4319.

SIDS, Screening Information Data Set, Initial Assessment Report for SIDS Initial Assessment Meeting (SIAM) 15, Triphenyl Phosphate (CAS 115–86-6) p.13 (October 2006). Available as of November 3, 2019: http://www.inchem.org/pages/sids.html).

Sierra A, Encinas JM, Deudero JJ, et al.2010. Microglia Shape Adult Hippocampal Neurogenesis through Apoptosis-Coupled Phagocytosis. Cell Stem Cell7:483–495. [PubMed: 20887954]

Sims JE, Smith DE2010. The IL-1 family: regulators of immunity. Nat. Rev. Immunol. 10(2):89–102. [PubMed: 20081871]

Sirenko O, Parham F, Dea S, et al.2019. Functional and Mechanistic Neurotoxicity Profiling Using Human iPSC-Derived Neural 3D Cultures. Toxicol. Sci. 167:58–76. [PubMed: 30169818]

Sjödin A, Patterson DG Jr.. Bergman A. 2003. A review on human exposure to brominated flame retardants—particularly polybrominated diphenyl ethers. Environ. Int. 29:829–839. [PubMed: 12850099]

Snider NT, Nast JA, Tesmer LA, et al.2009. A Cytochrome P450-Derived Epoxygenated Metabolite of Anandamide Is a Potent Cannabinoid Receptor 2-Selective Agonist. Mol. Pharmacol. 75:965–972. [PubMed: 19171674]

Sominsky L, De Luca S, Spencer SJ2018. Microglia: key players in neurodevelopment and neuronal plasticity. Int. J. Biochem. Cell Biol. 94:56–60. [PubMed: 29197626]

Stapleton HM, Klosterhaus S, Eagle S, et al.2009. Detection of organophosphate flame retardants in furniture foam and US house dust. Environ. Sci. Technol. 43:7490–7495. [PubMed: 19848166]

Stockholm Convention on Persistent Organic Pollutants. 2017. Accessed 4/14/2020. http://chm.pops.int/TheConvention/Overview/TextoftheConvention/tabid/2232/Default.aspx

Strowig T, Henao-Mejla J, Elinav E, et al.2012. Inflammasomes in health and disease. Nature481:278–286. [PubMed: 22258606]

Stutz A, Horvath GL, Monks BG, et al.2013. ASC speck formation as a readout for inflammasome production. Meth. Mol. Biol. 1040:91–101.

Suh KS, Choi EM, Rhee SY, et al.2017. Tetrabromobisphenol a induces cellular damages in pancreatic β-cells in vitro. J. Environ. Sci. Hlth, Part A52:624–631.

Szychowski KA, Wójtowicz AK2016. TBBPA causes neurotoxic and the apoptotic responses in cultured mouse hippocampal neurons in vitro. Pharmacol. Rep. 68:20–26. [PubMed: 26721346]

Takeshita T, Watanabe W, Toyama S, et al.2013. Effect of brazilian propolis on exacerbation of respiratory syncytial virus infection in mice exposed to tetrabromobisphenol, a brominated flame retardant. Evid. Based Complement Alternat. Med. 2013:698206. doi: 10.1155/2013/698206

Thion MS, Garel S. 2017. On place and time: Microglia in embryonic and perinatal brain development. Curr. Opin. Neurobiol. 47:121–130. [PubMed: 29080445]

Thomsen C, Lundanes E, Becher G. 2002. Brominated flame retardants in archived serum samples from Norway: A study on temporal trends and the role of age. Environ Sci Technol36(7):1414–1418. [PubMed: 11999045]

van der Veen I, de Boer J. 2012. Phosphorus flame retardants: Properties, production, environmental occurrence, toxicity and analysis. Chemosphere88:1119–1153. [PubMed: 22537891]

Venegas C, Kumar S, Franklin BS, et al.2017. Microglia-derived ASC specks cross-seed amyloid-β in Alzheimer's disease. Nature552:355–361. [PubMed: 29293211]

Wang D, Zhu W, Chen L, et al.2018. Neonatal triphenyl phosphate and its metabolite diphenyl phosphateexposure induce sex- and dose-dependent metabolic disruptions in adult mice. Environ. Pollution237:10–17.

Watanabe W, Hirose A, Takeshita T, et al.2017. Perinatal exposure to tetrabromobisphenol A (TBBPA), a bromated flame retardant, exacerbated the pneumonia in respiratory syncytial virus (RSV)-infected offspring mice. J.Toxicol. Sci. 42:789–795.

Wojtowicz AK, Szychowski KA, Kajta M. 2014. PPAR-γ agonist GW1929 but not antagonist GW9662 reduces TBBPA-induced neurotoxicity in primary neocortical cells. Neurotox. Res. 25:311–322. [PubMed: 24132472]

Yasmin S, Whalen M. 2018. Flame retardants, hexabromocyclododecane (HCBD) and tetrabromobisphenol A (TBBPA), alter secretion of tumor necrosis factor alpha (TNFα) from human immune cells. Arch. Toxicol. 921483–1494.

Ye G, Chen Y, Wang H, et al.2016. Metabolomics approach reveals metabolic disorders and potential biomarkers associated with the developmental toxicity of tetrabromobisphenol A and tetrachlorobisphenol A. Sci. Rep. 6:3525710.1038/srep35257 [PubMed: 27734936]

Zheng X, Xu R, Chen K, et al.2015. Flame retardants and organochlorines in indoor dust from several e-waste recycling sites in South China: composition variations and implications for human exposure. Environ. Int. 78, 1–7 (2015). doi: 10.1016/j.envint.2015.02.006. [PubMed: 25677852]

Zhou R, Yazdi AS, Menu P, et al.2011. A role for mitochondria in NLRP3 inflammasome activation, Nature469:221–225. [PubMed: 21124315]

Zieminska E, Lenart J, Diamandakis D, et al.2017. The role of The Role of Ca_{2+} Imbalance in the Induction of Acute Oxidative Stress and Cytotoxicity in Cultured Rat Cerebellar Granule Cells Challenged with Tetrabromobisphenol A. Neurochem. Res. 42:777–787. [PubMed: 27718046]

Zieminska E, Stafiej A, Toczylowska B, et al.2015. Role of Ryanodine and NMDA Receptors in Tetrabromobisphenol A-Induced Calcium Imbalance and Cytotoxicity in Primary Cultures of Rat Cerebellar Granule Cells. Neurotox. Res. 28:195–208. [PubMed: 26215658]

Highlights

1. PBP, TBBPA, or TPP exposure modified mitochondrial bioenergetics of microglia
2. PBP and TBBPA showed potential as trigger for NLRP3 inflammasome activatio.
3. PBP and TBBPA diminished phagocytic capability
4. FR exposure did not inhibit response to LPS

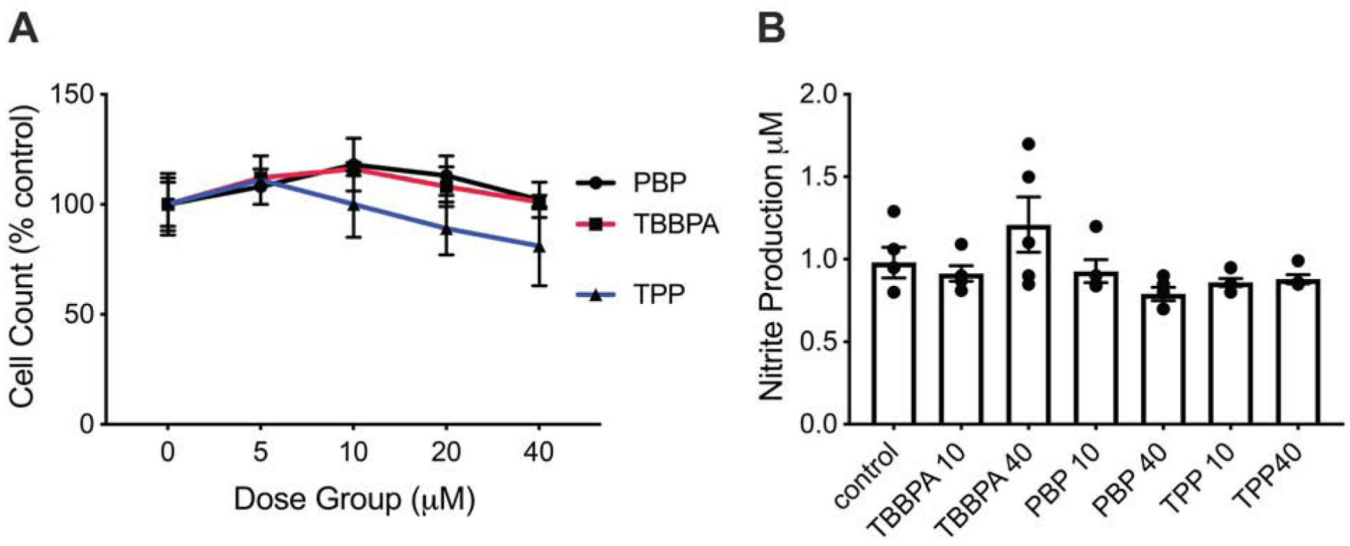

Figure 1.

A. Cell viability of BV-2 cells following 18 hr post-exposure to PBP, TBBPA, or TPP at various concentrations. Data represents total cell count (mean +/− SEM) as % of controls (n=4). B. Nitrite accumulation in BV-2 cells following 18 hr exposure to FRs at 10 μM or 40 μM for 18 hr as determined by Greiss assay. Data represents individual values and mean +/− SEM (n=5).

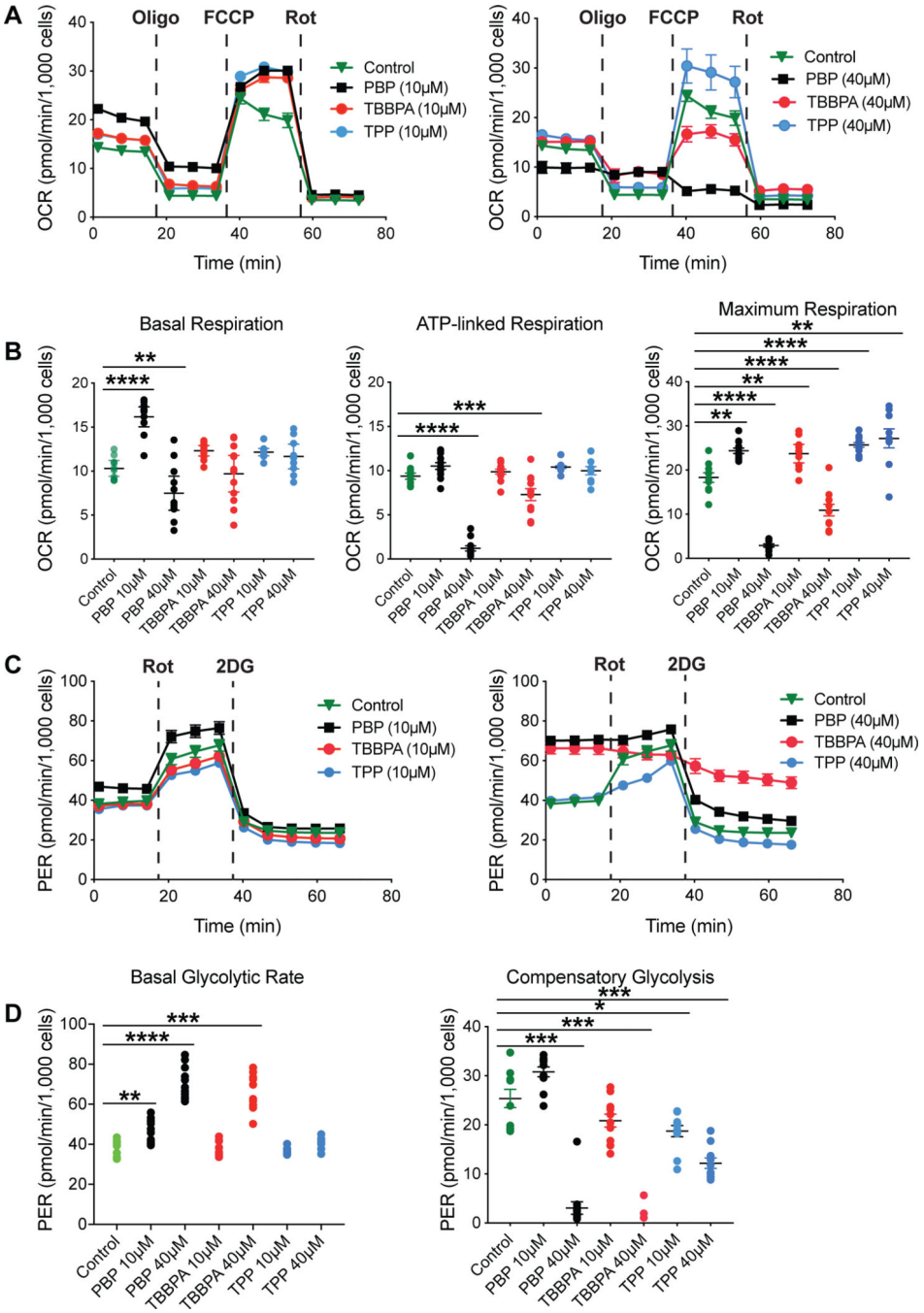

Figure 2.

A. Representative mitochondrial bioenergetics profile of BV-2 cells exposed to vehicle or PBP, TBBPA, or TPP at 10 (left image) or 40 μM (right image) for 18 hr. After signal stabilization (three measures) cells were sequentially exposed to the mitochondrial stressors: oligomycin (Oligo), FCCP, and rotenone (Rot). B. Basal respiration was significantly increased with 10μM PBP and decreased at 40 μM. ATP-linked respiration was significantly decreased at 40 μM PBP and TBBPA. Maximum respiration was significantly altered for all FRs at all exposure levels. C. Representative glycolytic profile of BV-2 cells exposed to

vehicle or PBP, TBBPA, or TPP at 10 or 40 μM. Cells were sequentially exposed to Rot and 2-deoxyglucose (2DG). D. Basal glycolytic rate was significantly increased for PBP at both exposure levels and for TBBPA at 40μM. With the exception of no change at PBP 10 μM, compensatory glycolysis was significantly decreased for all FRs at both exposure levels. A,C data represents mean response (n=9); B,D data represents individual values and median (n=9). * $p<0.05$; ** $p<0.01$; *** $p<0.001$; **** $p<0.0001$.

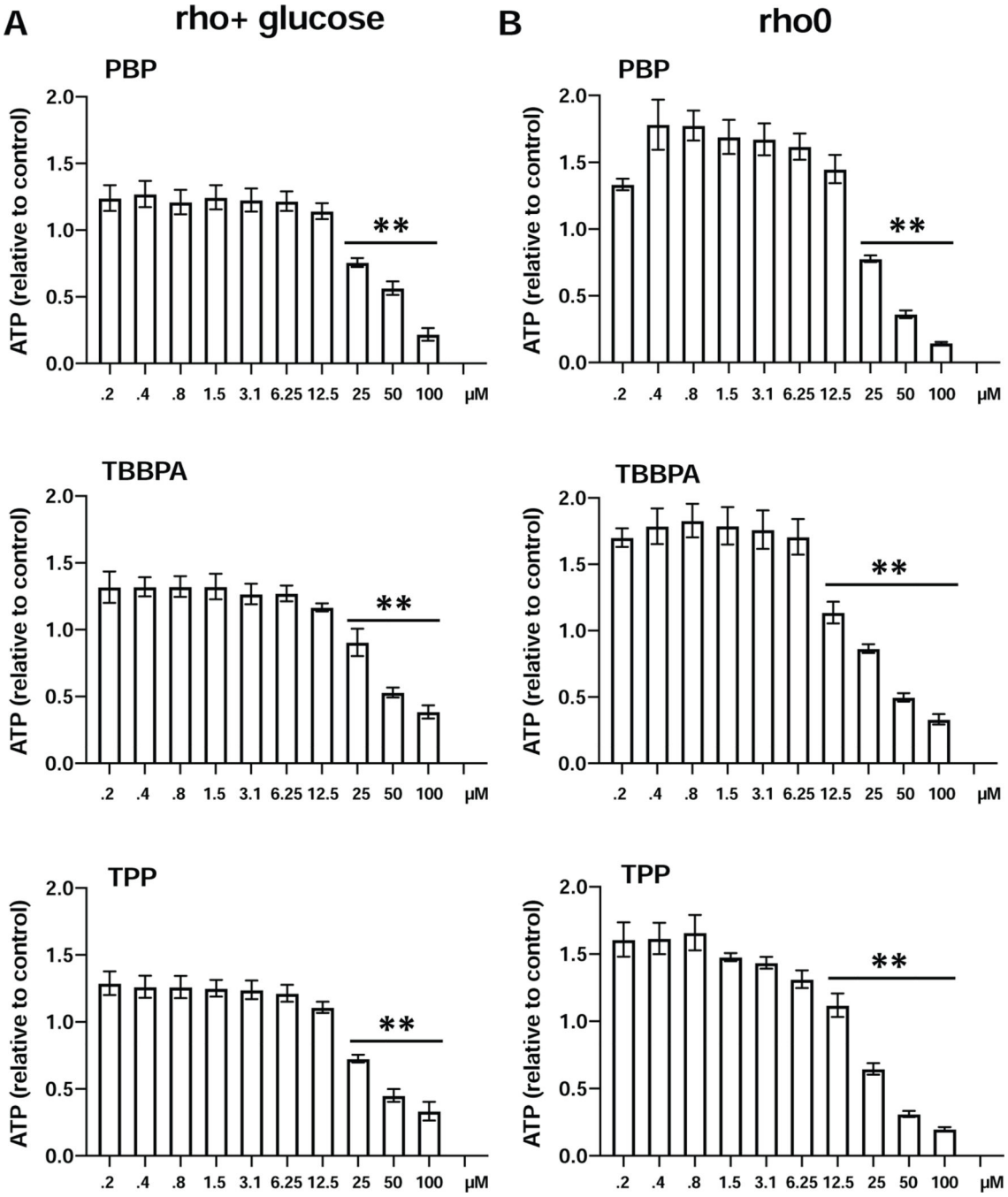

Figure 3.

ATP levels (Cell-Titer-Glo) in 2 isogenic osteosarcoma cell lines (143B) that either carry the full complement of mitochondrial DNA (rho+) or that have been depleted from the mtDNA (rho0) by chronic exposure to 50 ng/mL of ethidium bromide. Cells were exposed to various concentration of PBP, TBBPA, or TPP for 24 hr. Data represents mean+/− SEM (n=3) relative to controls. *** $p<0.01$.

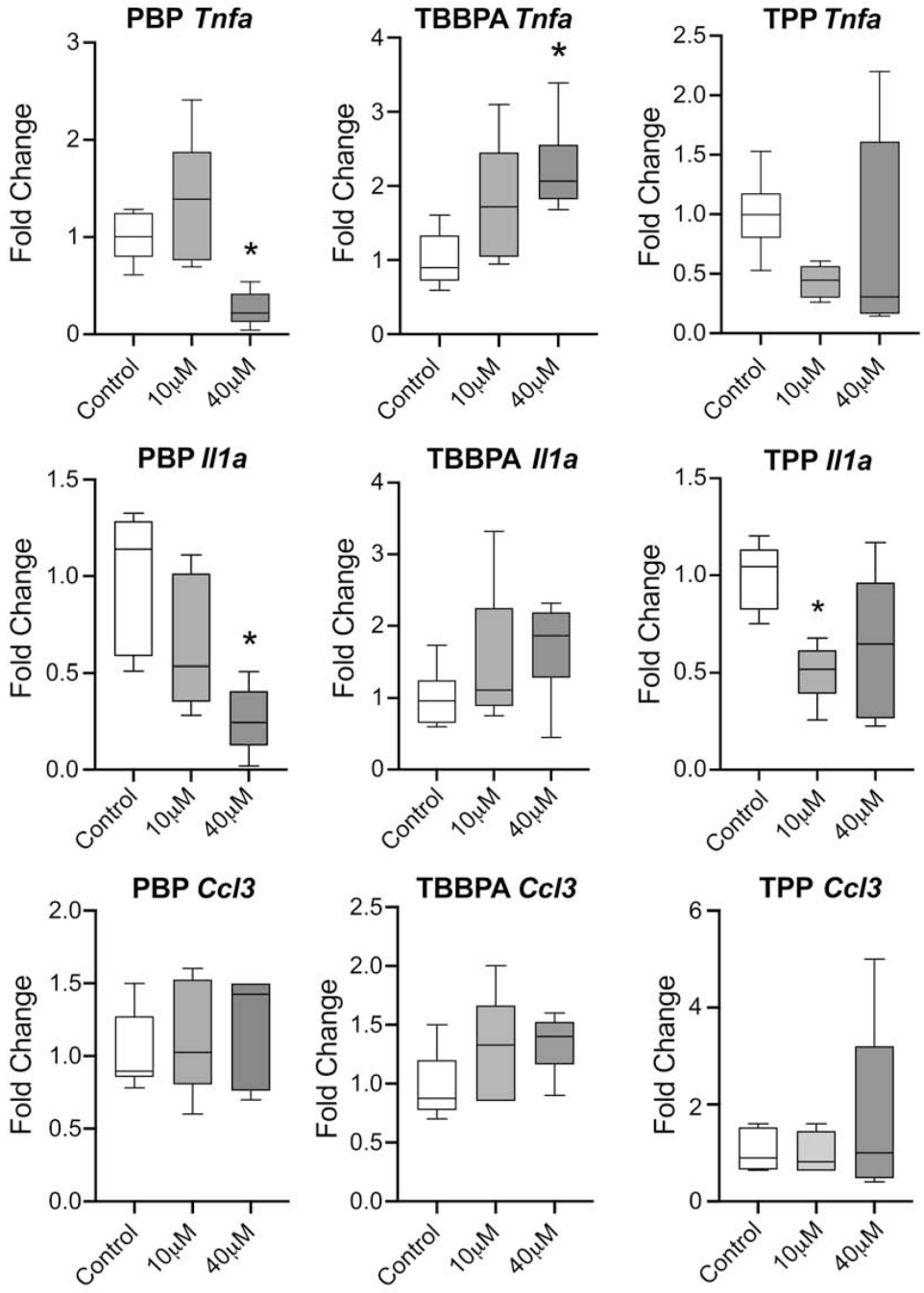

Figure 4.

A. *Tnfa, Il1a*, and *Ccl3* mRNA levels in BV-2 cells following 18 hr exposure to PBP, TBBPA, or TPP at 10 or 40 μM determined by qRT-PCR using TaqMan®. Relative gene expression amounts normalized to GAPDH and presented as fold change from control. B. Data was analyzed by a one-way ANOVA for each FR followed by Dunnett's tests for independent group mean comparisons. Data represents (n=6). *p<0.05

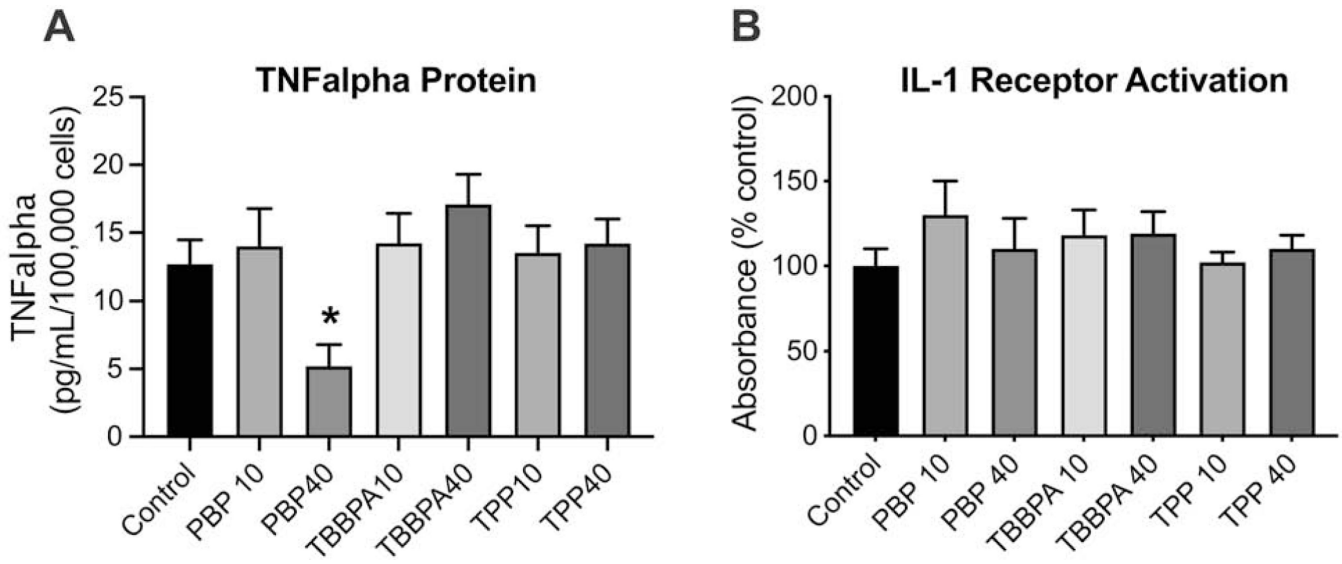

Figure 5.

A. TNFα protein levels determined by ELISA (n=6) and B. Production of IL-1 protein as detected by HEK Blue™ IL-1R cells (InvivoGen, San Diego, CA) (n=9) by BV-2 cells following exposure to PBP, TBBPA, or TPP at 10μM or 40 μM. Data represents mean +/− SEM. *p<0.05

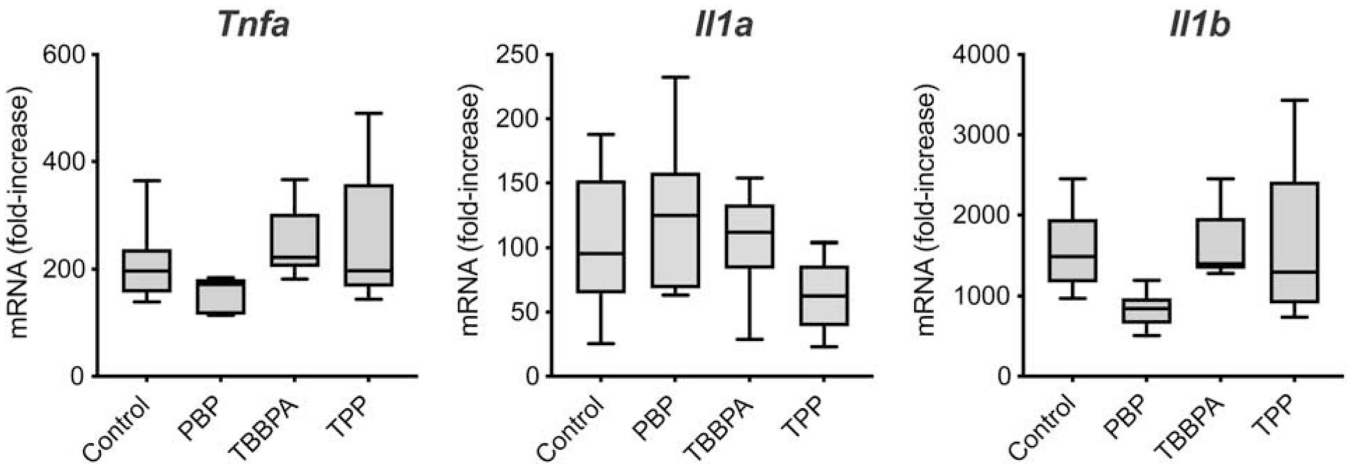

Figure 6.

LPS induction of *Tnfa, Il1a*, and *Il1b* mRNA levels over 3 hr in BV-2 cells exposed for a total of 18 hr to 10 μM PBP, TBBPA, or TPP. Data represents fold change over non-LPS dosed cells. (n=6).

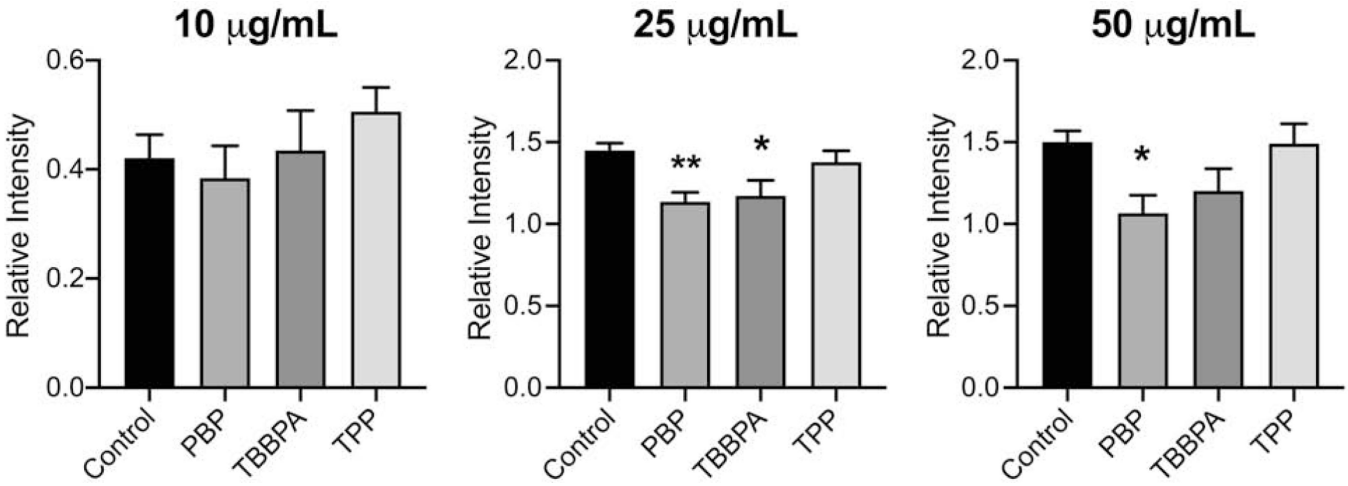

Figure 7.

Phagocytosis of bioparticles (10, 25, or 50 μg/mL) in BV-2 cells following exposure to PBP, TBBPA, or TPP at 10μM for 18hr. Cells were visualized (ImageXpress™ Micro Confocal; Molecular Devices, San Jose, CA) and quantitation of phagocytic uptake in Iba-1+ cells was conducted on 4 defined regions within each well. The average ratio of fluorescent intensity to cells was calculated for each well using MetaXpress software. Data represents mean of each well+/− SEM (n= 4). *p<0.05

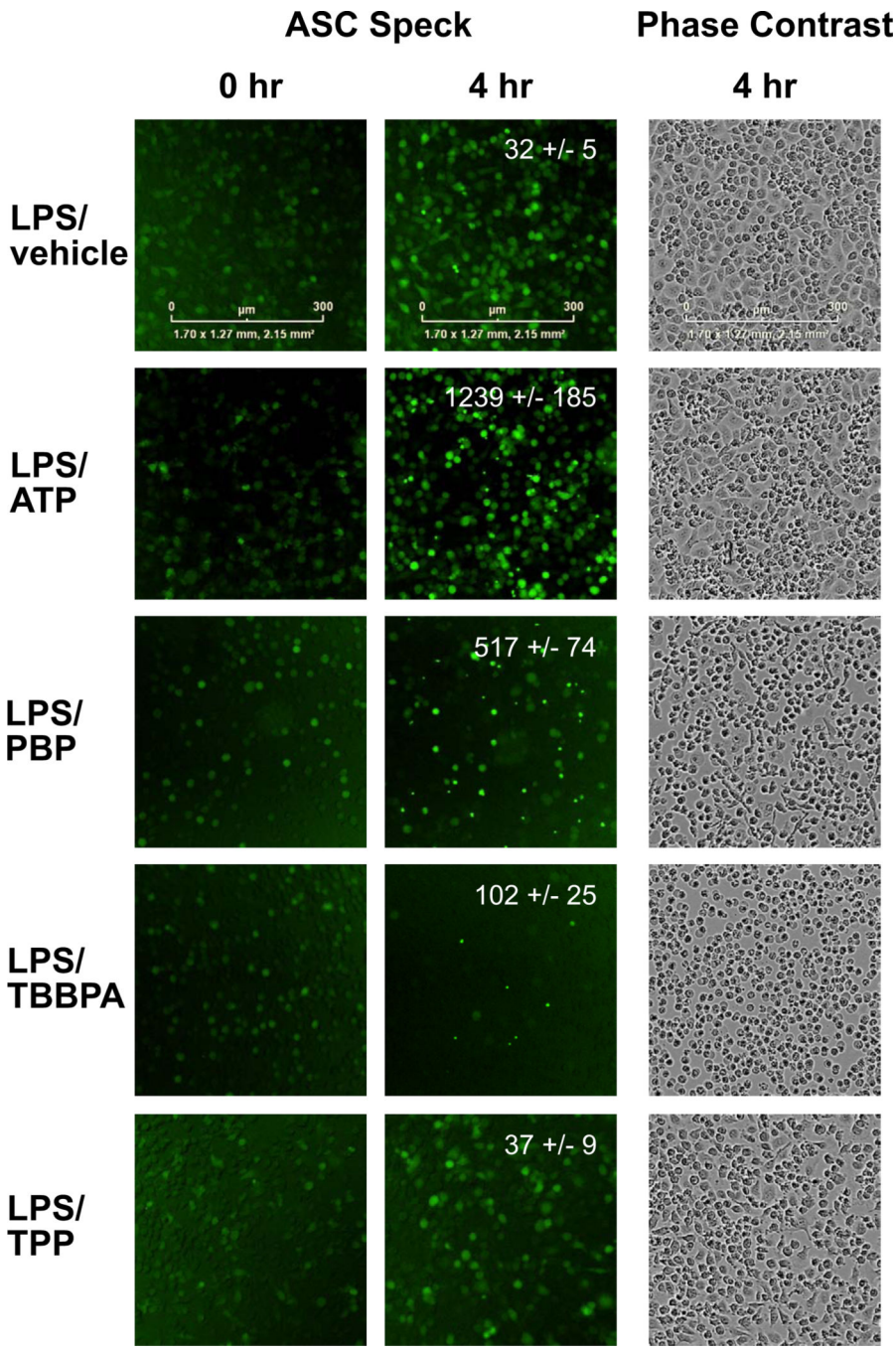

Figure 8.

Representative images of BV-2 ASC Speck cells and inflammasome activation over 4 hr. Images were captured an IncuCyte S3 live-cell analysis system and IncuCyte ZOOM 2015A software. Regions of interest (ROI) were identified within each well, standardized by total number of cells, threshold set for Speck size and intensity, and the number of ASC SPECKS (fluorescent aggregates) within each ROI determined using Fiji ImageJ software. Data represents mean +/− SEM (n=6).